



1 **Sources and atmospheric processing of wintertime aerosols**  
2 **in Seoul, Korea: Insights from real-time measurements using**  
3 **a high-resolution aerosol mass spectrometer**

4 **Hwajin Kim<sup>1,2</sup>, Qi Zhang<sup>3,4\*</sup>, Gwi-Nam Bae<sup>1,2</sup>, Jin Young Kim<sup>1,2</sup>, Seung Bok Lee<sup>1,2</sup>**

5 [1] Center for Environment, Health and Welfare Research, Korea Institute of Science and  
6 Technology, Seoul, Korea

7 [2] Department of Energy and Environmental Engineering, University of Science and Technology,  
8 Daejeon, Korea

9 [3] Department of Environmental Toxicology, University of California, Davis, CA 95616, USA

10 [4] Department of Environmental Science and Engineering, Fudan University, Shanghai, China.

11

12 \*Corresponding author: Qi Zhang

13 Department of Environmental Toxicology, University of California 1 Shields Avenue, Davis,  
14 California 95616

15 Phone: (530)-752-5779

16 Email: [dkwzhang@ucdavis.edu](mailto:dkwzhang@ucdavis.edu)

17

18 **Abstract**

19 Highly time-resolved chemical characterization of non-refractory submicrometer particulate  
20 matter (NR-PM<sub>1</sub>) was conducted in Seoul, the capital and largest metropolis of Korea, using an  
21 Aerodyne high-resolution time-of-flight aerosol mass spectrometer (HR-ToF-AMS). The  
22 measurements were performed during winter, when elevated particulate matter (PM) pollution  
23 events are often observed. This is the first time that detailed real-time aerosol measurement results  
24 are reported from Seoul, Korea, which reveal valuable insights into the sources and atmospheric  
25 processes that contribute to PM pollution in this region.



1           The average concentration of submicron aerosol ( $PM_{10} = NR-PM_{10} + \text{black carbon (BC)}$ ) was  
2  $27.5 \mu\text{g m}^{-3}$ , and the total mass was dominated by organics (44%), followed by nitrate (24%) and  
3 sulfate (10%). The average atomic ratios of oxygen-to-carbon (O/C), hydrogen-to-carbon (H/C),  
4 and nitrogen-to-carbon (N/C) of organic aerosol (OA) were 0.37, 1.79, and 0.022, respectively,  
5 which gives that average organic mass-to-carbon (OM/OC) ratio of 1.67. The concentrations ( $2.6\text{--}$   
6  $90.7 \mu\text{g m}^{-3}$ ) and composition of  $PM_{10}$  varied dynamically during the measurement period, due to  
7 the influences of different meteorological conditions, emission sources, and air mass origins. Five  
8 distinct sources of OA were identified via positive matrix factorization (PMF) analysis of the HR-  
9 ToF-AMS data: vehicle emissions represented by a hydrocarbon like OA factor (HOA; O/C =  
10 0.06), cooking activities represented by a cooking OA factor (COA; O/C = 0.15), wood  
11 combustion represented by a biomass burning OA factor (BBOA; O/C = 0.34), and secondary  
12 organic aerosol (SOA) represented by a semi-volatile oxygenated OA factor (SV-OOA; O/C =  
13 0.56) and a low volatility oxygenated OA factor (LV-OOA; O/C = 0.68). On average, primary OA  
14 ( $POA = HOA + COA + BBOA$ ) accounted for 59% the OA mass whereas SV-OOA and LV-OOA  
15 contributed 15% and 26%, respectively.

16           Our results indicate that air quality in Seoul during winter is influenced strongly by  
17 secondary aerosol formation with sulfate, nitrate, ammonium, SV-OOA, and LV-OOA together  
18 accounting for 64% of the  $PM_{10}$  mass during this study. However, aerosol sources and composition  
19 were found to be significantly different between clean and polluted periods. During stagnant  
20 periods with low wind speed (WS) and high relative humidity (RH), PM concentration was  
21 generally high (average  $\pm 1\sigma = 43.6 \pm 12.4 \mu\text{g m}^{-3}$ ) with enhanced fractions of nitrate (27%) and  
22 SV-OOA (8%), which suggested a strong influence from local production of secondary aerosol.  
23 Low PM loading periods ( $12.6 \pm 7.1 \mu\text{g m}^{-3}$ ) tended to occur under higher WS and lower RH  
24 conditions and appeared to be more strongly influenced by regional air masses, as indicated by  
25 higher mass fractions of sulfate (12%) and LV-OOA (21%) in  $PM_{10}$ . Overall, our results indicate  
26 that PM pollutants in urban Korea originate from complex emission sources and atmospheric  
27 processes and that their concentrations and composition are controlled by various factors including  
28 meteorological conditions, local anthropogenic emissions, and upwind sources.

29



## 1 **1 Introduction**

2 Ambient aerosols can reduce visibility, damage human health, and influence climate change  
3 directly by absorbing and reflecting solar radiation, and indirectly by modifying cloud formation  
4 and properties (IPCC, 2013; Pope III and Dockery, 2006; Pöschl, 2005). Elevated particulate matter  
5 (PM) pollution in urban areas are known to arise due to anthropogenic emissions and stagnant  
6 meteorological conditions (Cao et al., 2012; Guo et al., 2014; Sun et al., 2014).

7 Seoul is one of the most populated and developed city in Korea and is facing a severe PM pollution  
8 problem. The annual average concentration of PM<sub>2.5</sub> in Seoul decreased from 28.5  $\mu\text{g m}^{-3}$  in 2005  
9 to 22.5  $\mu\text{g m}^{-3}$  in 2012 since the enactment of the “Special Act on Seoul Metropolitan Air Quality  
10 Improvement” in 2005, which has led to emission reduction from diesel vehicles and fugitive dust  
11 emissions on road and open area (Kang et al., 2016; KOSAE, 2009). However, the amount of  
12 reduction was not dramatic and the annual average PM<sub>2.5</sub> concentration increased again in 2013 to  
13 24.8  $\mu\text{g m}^{-3}$ . These values far exceeded the PM<sub>2.5</sub> annual standards set by the USA (15  $\mu\text{g m}^{-3}$ ) and  
14 the WHO (10  $\mu\text{g m}^{-3}$ ). Due to growing concerns over the adverse effects of atmospheric PM, the  
15 South Korean government established PM<sub>2.5</sub> standards in 2015: 25  $\mu\text{g m}^{-3}$  for annual average and  
16 50  $\mu\text{g m}^{-3}$  for 24-hr average (NIER, 2014).

17 Mitigating air pollution in Seoul remains a great challenge because it remains unclear which  
18 emission sources and atmospheric process are responsible for the problem (Harrison and Yin,  
19 2000), despite numerous studies that have focused on these issues worldwide (e.g., Ervens et al.,  
20 2011; Gelencsér et al., 2007; Jimenez et al., 2009; Ng et al., 2010; Young et al., 2016; Zhang et al.,  
21 2007a). A main reason is the complexity of ambient aerosols, which have a range of chemical  
22 compositions and originate from a wide range of sources and atmospheric processes (Seinfeld and  
23 Pandis, 2006). Furthermore, several recent studies investigate the impacts of meteorology on air  
24 pollution, as well (Ding et al., 2013; Ding et al., 2016; Petaja et al., 2016). For example, high PM  
25 concentration was found to happen more frequently during winter due to a combination of factors,  
26 including elevated emissions from primary sources for heating, lower boundary layer (BL) height,  
27 and stagnant meteorological conditions, which favor the accumulation of PM and secondary  
28 aerosol precursors. In addition, cold weather in winter promotes the gas-to-particle partitioning of  
29 semi-volatile species such as nitrate. In addition, since Seoul is located downwind from the Asian  
30 Continent, where concentrations of ambient aerosols have increased significantly in recent years  
31 (Huang et al., 2014; Liu et al., 2013; Quan et al., 2011), long-range transport of pollutants from



1 upwind polluted areas often influences air quality in Seoul, especially during winter (Kim et al.,  
2 2014). As a result, both local and regional sources contribute to high concentrations of PM, both  
3 separately and in combination (Heo et al., 2009), making air quality control more difficult.  
4 Therefore, understanding the sources and processes responsible for PM composition and  
5 concentration is critical for the public to recognize regional haze events and to enact effective PM  
6 reduction strategies for Korea as well as for the broader northern pan-Eurasian region (Liu et al.,  
7 2013). Also, from a global point of view, studies of atmospheric PM pollution may contribute to  
8 a better understanding of the Earth system science and enacting efficient climate policy (Kulmala  
9 et al., 2015).

10 Most previous aerosol studies in Korea were based on offline sampling which involves filter  
11 collection followed by laboratory analyses. However, a main drawback of this method is low time-  
12 resolution which limits our ability to perform detail investigations on the atmospheric evolution  
13 processes. Furthermore, organic aerosol (OA) analysis conducted in Korea has so far focused on  
14 molecular level, which led to the identification of a small portion of the OA mass (Choi et al.,  
15 2012;Choi et al., 2016). Aerosol mass spectrometers (AMS) have been widely used in recent years  
16 because they allow for chemical speciation, sizing and the mass detection of submicron non-  
17 refractory submicrometer particulate matter (NR-PM<sub>1</sub>), with a high time resolution (Canagaratna  
18 et al., 2007). Furthermore, using multivariate analysis methods (Zhang et al., 2011), the OA was  
19 decomposed into several sources such as hydrocarbon-like OA (HOA), biomass burning OA  
20 (BBOA), cooking-related OA (COA), coal combustion OA (CCOA), and oxygenated OA (OOA).  
21 In addition, the OOA factor has been further separated according to volatility, e.g., low volatility  
22 fraction (LV-OOA) and a semi-volatile fraction (SV-OOA) or oxidation, e.g., more oxidized (MO-  
23 OOA) and less oxidized (LO-OOA) (e.g., Lanz et al., 2007;Parworth et al., 2015;Setyan et al.,  
24 2012;Aiken et al., 2008;Huang et al., 2011;Mohr et al., 2012). These studies have identified the  
25 sources, constituents and the evolution process of PM which is critical for establishing efficient  
26 control strategies and model representations (Ulbrich et al., 2009;Zhang et al., 2011).

27 Many AMS studies have been conducted in East Asia including China, Hong Kong, and Japan,  
28 but a detailed PM characterization using AMS has not yet been reported in Seoul, Korea (Li et al.,  
29 2015 and references therein). In this study, we deployed a high-resolution time-of-flight aerosol  
30 mass spectrometer (HR-ToF-AMS), manufactured by Aerodyne Research Inc. (BillERICA, MA,  
31 USA), in Seoul for 6 weeks (from December 5, 2015 to January 21, 2016) to characterize



1 wintertime NR-PM<sub>1</sub> in this urban area. We particularly focus on aerosol properties, sources, and  
2 processes in winter, when the weather was generally cold and relatively dry during the day but was  
3 humid during the night. Our goal was to use detailed information obtained from in situ  
4 measurements to facilitate a fundamental understanding of the formation processes and emission  
5 sources of atmospheric aerosols in Seoul, which may improve our understandings on what factors  
6 and how they influences urban air quality. This information will eventually allow for the design  
7 of better pollution abatement strategies and improved parameterizations in air quality models. Here,  
8 we report: (1) the mass concentrations, size distributions, chemical composition, and temporal and  
9 diurnal variations of PM<sub>1</sub> species; (2) the characteristics and dynamic variations of OA sources  
10 and processes using PMF; and (3) the characteristics, sources, and impact factors of the PM<sub>1</sub>  
11 composition and OA components on polluted and unpolluted days.

12

## 13 **2 Experimental Methods**

### 14 **2.1 Sampling site description**

15 Seoul, the capital of Korea, is located in the central-west of the Korean Peninsula surrounded by  
16 the Yellow Sea. Korea is generally under the influence of a prevailing north-westerly wind  
17 bringing air masses originating from mainland China during winter (Fig. 1). In this study, real-  
18 time measurements of particle composition and size distribution were conducted at the Korea  
19 Institute of Science and Technology (KIST) located in the northeast of Seoul (37.60N, 127.05E),  
20 7 km from the city center. The sampling was conducted on the 5<sup>th</sup> floor of one of the KIST  
21 buildings (60 m above sea level). As shown in Fig. 1d, KIST is located ~ 400 m from a busy  
22 highway and is surrounded by a residential area, forest and a commercial area, suggesting that the  
23 air quality at the site tends to be influenced by abundant anthropogenic and primary sources. There  
24 are no major industrial or wood burning sources in the vicinity of KIST. However, in the west and  
25 west south part of Seoul, ~ 35 km away from the measurement site (Fig. 1b), there are a number  
26 of industrial facilities that are significant anthropogenic sources. There are also sporadic  
27 agricultural areas surrounding the city of Seoul (e.g., Gyeonggi), where open biomass burning  
28 often times occurs during winter. A wide range of meteorological and air quality data were also  
29 collected from a separate supersite located at 500 m away from the northwest of the KIST.



## 1 2.2 Measurements

2 The NR-PM<sub>1</sub> chemical components including sulfate, nitrate, ammonium, chloride, and organics  
3 as well as their size distributions were measured by an Aerodyne HR-ToF-AMS (DeCarlo et al.,  
4 2006) at a time resolution of 2.5 min. The black carbon (BC) concentration was measured with a  
5 multi angle absorption photometer (MAAP; Thermo Fisher Scientific, Waltham, MA, USA). Both  
6 instruments sampled downstream of a PM<sub>2.5</sub> cyclone (URG Corp.; Chapel Hill, NC, USA). The  
7 number size distributions of aerosols with mobility sizes between 20.9–947.5 nm were measured  
8 by a scanning mobility particle sizer (SMPS 3080; TSI Inc., St Paul, MN, USA). The hourly  
9 concentration of trace gas (e.g., CO, O<sub>3</sub>, NO<sub>2</sub> and SO<sub>2</sub>) measured at Gireum site (37.61N, 127.03E)  
10 were acquired from the Korea Environment Cooperation (KECO) (<http://www.airkorea.or.kr>).  
11 Meteorological measurement data such as ambient temperature, relative humidity (RH), wind  
12 speed and wind direction were obtained from the nearby Jungreung site (37.61N, 127.00E)  
13 maintained by the Korea meteorological administration (<http://www.kma.go.kr>). The data reported  
14 in this paper are in local time, which is Korea Standard Time (KST) and is 9 h earlier than the  
15 Universal Coordinated Time (UTC).

16 In this study, the HR-ToF-AMS was operated in the standard configuration and obtained mass  
17 spectra (MS) and efficient particle time of flight (ePToF) data. Furthermore, the HR-ToF-AMS  
18 was operated under the ‘V’ and ‘W’ modes, where high sensitivity but low mass resolution was  
19 achieved in ‘V’ mode, and low sensitivity, but high mass resolution was achieved in ‘W’ mode.  
20 Ionization efficiency (IE) and particle sizing calibrations were performed following standard  
21 protocols (Canagaratna et al., 2007) before, during, and after the measurement period.

## 22 2.3 AMS data analysis

### 23 2.3.1 Basic HR-ToF-AMS data analysis

24 HR-ToF-AMS data were processed and analyzed using the standard toolkit (SeQUential Igor data  
25 RetRiEval (SQUIRREL; ver. 1.57I), and PIKA (ver. 1.16H; available for download at  
26 <http://cires.colorado.edu/jimenez-group/ToFAMSResources/ToFSoftware/index.html>)) within  
27 Igor Pro (Wavemetrics, Lake Oswego, OR, USA). Details on the data processing procedures have  
28 been described in previous studies (Aiken et al., 2008; Aiken et al., 2009; Allan et al., 2004).  
29 Briefly, the standard fragmentation table described by Allan et al. (2004) was used, with some  
30 small modifications to process the raw MS. The modifications were based on data from four



1 filtered air measurements. This allowed measurements of the background from the gas-phase  
2 signal, which needed to be removed from the particle-phase measurement. Adjustments were made  
3 to the measured  $\text{CO}_2^+$  ( $m/z = 44$ ) signal to remove the contributions from gas phase  $\text{CO}_2$  as well  
4 as the  $^{16}\text{O}^+$  to  $^{14}\text{N}^+$  ratio for air signals at  $m/z = 29$  based on measurements of particle-free ambient  
5 air. Relative ionization efficiencies (RIE) of 1.1, 1.075, and 3.875 were used for nitrate, sulfate,  
6 and ammonium, respectively, based on values determined from calibrations using pure  $\text{NH}_4\text{NO}_3$   
7 and  $(\text{NH}_4)_2\text{SO}_4$  aerosols. A composition-dependent collection efficiency (CDCE) was applied to  
8 the data based on an algorithm by Middlebrook et al. (2012). Nitrate was observed to be an  
9 important component of NR- $\text{PM}_{10}$  during this study (24%), although the campaign average ( $\pm 1\sigma$ )  
10 CE was  $0.5 \pm 0.02$ .

11 The quantification of NR- $\text{PM}_{10}$  species was validated through comparisons between the total  $\text{PM}_{10}$   
12 mass ( $\text{PM}_{10} = \text{NR-PM}_{10} + \text{BC}$ ) and the apparent particle volume measured by the SMPS (Fig. 2e,  
13 Fig. S1a). As shown in Fig. S1a, the SMPS-measured particle volume correlated strongly with the  
14 AMS measured total mass ( $R^2 = 0.9$ ). From this strong correlation, the inter-comparison of AMS  
15 mass versus SMPS volume yielded a slope of 1.22, which was lower than the average particle  
16 density of 1.46 estimated using the measured chemical composition in this study (Zhang et al.,  
17 2005b) (Fig. 3c and Fig. S1b). Note that the average organic aerosol density was estimated to be  
18 1.12 based on elemental ratios (Kuwata et al., 2012). The evolution pattern of the AMS total mass-  
19 based size distribution also compared well with the volume-based size distribution from SMPS  
20 measurements throughout the day (Fig. S1c,d). The detection limits of the main chemical  
21 components in AMS are listed in Table 1, and are typically far lower than the observed  
22 concentrations. All the reported mass concentrations from AMS in this study are based on ambient  
23 conditions.

24 The elemental ratios between oxygen, carbon, hydrogen, and nitrogen as well as the organic mass  
25 to carbon ratio (OM/OC) of OA, were determined from an analysis of the W mode high resolution  
26 mass spectra (HRMS) data, following the method recently reported by Canagaratna et al. (2015).  
27 The elemental ratios calculated using the Aiken-Ambient method (Aiken et al., 2008) are detailed  
28 in Table S1 along with the ratios calculated using the Canagaratna method for comparison. Unless  
29 otherwise indicated, the O/C, H/C, and OM/OC ratios stated in this paper from other studies have  
30 been calculated using the updated elemental analysis method (Canagaratna et al., 2015).

### 31 2.3.2 Positive Matrix Factorization (PMF) Analysis



1 The HRMS of organic aerosol were analyzed using PMF. The analysis was performed using the  
2 PMF2 algorithm in robust mode (Paatero and Tapper, 1994), with the PMF Evaluation Toolkit  
3 (PET ver 2.05) (Ulbrich et al., 2009), which was downloaded from  
4 [http://cires1.colorado.edu/jimenez-group/wiki/index.php/PMF-](http://cires1.colorado.edu/jimenez-group/wiki/index.php/PMF-AMS_Analysis_Guide#PMF_Evaluation_Tool_Software)  
5 [AMS\\_Analysis\\_Guide#PMF\\_Evaluation\\_Tool\\_Software](http://cires1.colorado.edu/jimenez-group/wiki/index.php/PMF-AMS_Analysis_Guide#PMF_Evaluation_Tool_Software). The data and error matrices were  
6 prepared according to the protocol described by Ulbrich et al. (2009) and outlined in Table 1 of  
7 Zhang et al. (2011). In brief, a minimum error value was applied to the error matrix and each ion  
8 was assessed and treated according to their signal-to-noise ratio (SNR). Ions with an average SNR  
9 of less than 0.2 were removed, and those with SNR between 0.2 and 2 were downweighted by  
10 increasing their errors by a factor of two. Further, ions related to  $m/z$  44 (i.e.,  $\text{CO}_2^+$ ,  $\text{CO}^+$ ,  $\text{H}_2\text{O}^+$ ,  
11  $\text{HO}^+$ , and  $\text{O}^+$ ) were also downweighted to avoid overestimating the importance of  $\text{CO}_2^+$ . Isotopes  
12 were removed from the matrices because their signals were scaled to their parent ions rather than  
13 being measured directly. After these treatments, the resulting matrix consisted of 286 ions between  
14  $m/z$ 's 12 and 120.

15 PMF was applied to the data and the number of factors ( $p$ ) in the solution was explored from one  
16 up to nine. Although the PMF algorithm was able to provide a number of mathematically sound  
17 solutions, in order to obtain physically meaningful results, several criteria were used to evaluate  
18 and select the appropriate number of factors from the model. The recommendations outlined in  
19 Zhang et al. (2011) including an investigation of the key diagnostic plots, mass spectral signatures,  
20 diurnal profiles, and correlations with external tracers, were followed to assess the results and  
21 determine the number of factors.

22 The rotational ambiguity of each of the solution sets was explored by varying the fPeak parameter  
23 from -1 to 1, with an increment of 0.1. The five factor solution with fPeak = 0 ( $Q/Q_{\text{exp}} = 2.56$ ), was  
24 selected for further analyses because it satisfied the above criteria, including a good separation of  
25 the temporal and mass spectral variations of the five factors. A summary of the key diagnostics is  
26 presented in Fig. S2 in the Supplement. The five factor solution was found to be very stable as the  
27 mass fraction of each of the factors remained relatively constant between fPeaks -0.4 and +0.2  
28 (Fig. S2c). Fig. S3 shows the mass spectra and the time series of the four and six factor solutions;  
29 where factor 1 and factor 2 in the four factor solution set could be identified as low volatility OA  
30 (LV-OOA) and semi-volatile OA (SV-OOA) based on the O/C ratio, but were both highly oxidized,  
31 with a higher fraction of  $m/z$  44 than  $m/z$  43. Moreover, all factors in this solution set showed the



1 signature of biomass burning OA (BBOA) at  $m/z$  60 and  $m/z$  73, indicating that more factors may  
2 be needed to resolve the mixed factors. In contrast, the temporal variations from the six factor  
3 solution were similar to those from the five factor solution set but showed indications of factor  
4 splitting. For example, two very similar BBOA-like factors (factors 3 and 4) were identified in the  
5 six factor solution, where the main difference was that factor 4 had a higher N/C ratio than factor  
6 3. Although different types of BBOA sources are possible, we did not have external evidence to  
7 validate the separation. Furthermore, given the fact that having only one BBOA factor (i.e., the  
8 five factor solution set) did not influence the separation of the other factors, it was not necessary  
9 to go for higher number of factors. Consequently, the five factor solution, which resolved HOA,  
10 COA, BBOA and two types of OOA, was chosen as it appears to best represent OA sources and  
11 processes in Seoul during winter.

## 12 **2.4 Backtrajectory and Bivariate conditional probability function analysis**

13 In this study, 96-h back trajectories were calculated every hour using version 4.8 of the Hybrid  
14 Single-Particle Lagrangian Integrated Trajectory (HYSPLIT) model (Draxler, 2012; Draxler, 1997)  
15 for the sampling periods from December 5, 2015 to January 21, 2016. The ending location for the  
16 trajectories was the KIST (latitude: 37.60N; longitude: 127.05E) at an elevation of 500m. To  
17 identify the pollutant characteristics in different predominant transport patterns, cluster analysis  
18 was performed on the trajectories using the software HYSPLIT4 and 4 clusters were identified  
19 according to their similarity in a spatial distribution.

20 In addition, conditional probability function (CPF) (Kim et al., 2003) was performed to estimate  
21 the local sources and their impacts on  $PM_{10}$  composition and individual organic aerosol sources  
22 from PMF analysis, using wind directions coupled with the concentration time series of each  
23 species. The CPF plots represent the probability that a specific compound or source is located in  
24 certain wind direction, assisting to find the local point source. The directional origin of regionally  
25 transported sources may not be consistent with the local surface wind data used for the CPF plots  
26 due to the topography of the region (Heo et al., 2009).

27

## 28 **3 Results and discussion**

### 29 **3.1 Overall characteristics**

#### 30 **3.1.1 Temporal variations of $PM_{10}$ composition and chemical properties**



1 The overall characteristics and temporal variations of wintertime  $PM_{10}$  in Seoul, including mass  
2 and volume concentrations, and size distributions are shown in Fig. 2, along with the time series  
3 of gaseous pollutants, e.g., CO, SO<sub>2</sub>, and O<sub>x</sub> (O<sub>x</sub> = O<sub>3</sub> + NO<sub>2</sub>), and meteorological conditions (RH,  
4 temperature, wind direction, wind speed). From Dec. 6, 2015 to Jan. 21, 2016, the average  
5 concentration of  $PM_{10}$  (= NR- $PM_{10}$  + BC) was 27.5  $\mu\text{g m}^{-3}$ , ranging from 2.6 to 90  $\mu\text{g m}^{-3}$ . Assuming  
6 that  $PM_{10}$  represents approximately 80% of  $PM_{2.5}$  mass (Lim et al., 2012), we found that 29% of  
7 the measurement days (i.e., 14 days) violated the NIER's daily  $PM_{2.5}$  standards (50  $\mu\text{g m}^{-3}$ ) and  
8 58% of the days (28 days) violated the WHO's daily standard (25  $\mu\text{g m}^{-3}$ ). Although severe haze  
9 with  $PM_{10}$  concentration close to 90  $\mu\text{g m}^{-3}$  was observed frequently, the averaged mass  
10 concentration of  $PM_{10}$  (27.5  $\mu\text{g m}^{-3}$ ) was still moderate because of the frequent occurrence of clean  
11 periods in winter. The average concentration of  $PM_{10}$  measured in Korea during this study was  
12 similar to or slightly lower than those measured during wintertime in several urban areas in China,  
13 including Shanghai (Huang et al., 2012), Shenzhen (He et al., 2011), Lanzhou (Xu et al., 2016),  
14 and Hong Kong (Li et al., 2015), but was much lower than in Beijing where the wintertime mass  
15 concentrations of  $PM_{10}$  were found to be 7-10 times higher than in Seoul (Sun et al., 2014).  
16 The large variations in  $PM_{10}$  mass concentrations (2.6 to 90  $\mu\text{g m}^{-3}$ ; Fig. 2e) and other pollutants  
17 (Fig. 2c), such as CO (0.3 to 2.3 ppm), O<sub>3</sub> (3 to 46 ppb), and NO<sub>2</sub> (8 to 98 ppb), reflected that air  
18 quality in Seoul is influenced by dynamic changes in emission sources, atmospheric processes, as  
19 well as meteorological conditions. In addition, new particle formation events were observed during  
20 this study and they showed characteristics of a sharp increase of ultrafine particle number  
21 concentration and subsequent growth of these particles in size (Fig.2i). This finding is the first  
22 time in urban area of Korea, although frequent (~7.4 % of the measurement days) observations of  
23 new particle formation and growth events were reported from the 3 year continuous measurements  
24 using SMPS at Gosan station (33.17N, 126.10E) which is pristine rural area but downwind site of  
25 Asian Continent facing yellow Sea (Kim et al., 2013).  
26 Based on the variations of  $PM_{10}$  concentrations and meteorological conditions (Fig. 2), we divided  
27 the whole study into two typical periods: (1) high loading period (daily  $PM_{10}$  > 30  $\mu\text{g m}^{-3}$ ) and (2)  
28 low loading period (daily  $PM_{10}$  < 14  $\mu\text{g m}^{-3}$ ). 30 and 14  $\mu\text{g m}^{-3}$  correspond to the middle values of  
29 the  $PM_{10}$  concentrations estimated based on the NIER and WHO daily and yearly  $PM_{2.5}$  standards,  
30 respectively. As shown in Figs. 2 and 3, high and low loading periods usually alternated during  
31 winter in Seoul. Comparisons between the high and low loading periods can indicate how different



1 sources and atmospheric processes influence air quality in this region. Details on the periodic  
2 variations of air quality in Seoul are discussed at section 3.4.

3 On average, OA was the largest component of the  $PM_{10}$ , accounting for 44% of the total mass,  
4 followed by nitrate (24%), sulfate (10%), ammonium (12%), BC (9%) and chloride (1%) (Fig. 3a,  
5 4a and Table 1). POA (= HOA + COA + BBOA) and SOA (= SV-OOA + LV-OOA) accounted  
6 for 59 and 41%, respectively, of OA mass (section 3.3). Consequently, ~ 36% of  $PM_{10}$  was consisted  
7 of primary materials (POA + BC), with the remainder (64%) being secondary species ( $NO_3^-$  +  
8  $SO_4^{2-}$  +  $NH_4^+$  + SOA), indicating that the aerosol pollution problem in Seoul during wintertime  
9 was more strongly influenced by secondary aerosol formation processes. Details on the sources  
10 and processes that led to severe air quality are discussed in section 3.4.

11 The molar equivalent ratios of total inorganic anions to cation for NR- $PM_{10}$  ( $= (SO_4^{2-}/48 + NO_3^-/62$   
12  $+ Cl^-/35.5) / (NH_4^+/18)$ ) were close to 1; thus, submicron aerosols were mostly neutralized in the  
13 forms of ammonium salts, such as  $NH_4NO_3$ ,  $(NH_4)_2SO_4$ , and  $NH_4Cl$  (Zhang et al., 2007b) (Figs.  
14 3d and 4b). Possible sources of ammonium in Seoul include on-road vehicle emissions, neutralizer  
15 using in industry, and agricultural emissions at the outskirts of Seoul. Note that particles appeared  
16 to have “excess”  $NH_4^+$  at high organic aerosol loadings (Fig. 4e), probably due to the presence of  
17 carboxylate ions, such as formate, acetate, and oxalate, which were not counted in the calculation  
18 of ion balance. Further investigations of this issue might be necessary in the future.

### 19 **3.1.2 Diurnal patterns of $PM_{10}$ composition**

20 Diurnal patterns can provide insights into aerosol sources and formation processes. In this study,  
21 the daily variations in concentrations of aerosol species show distinctively different patterns,  
22 indicating that the sources and formation processes of PM pollutants in Seoul were diverse and  
23 complex. First, secondary inorganic species, such as sulfate, nitrate, and ammonium, all displayed  
24 different diurnal profiles. In the case of nitrate (Fig. 5c), the daily variations started to increase at  
25 ~ 07:00, peaked at midday (10:00-12:00), and then slowly decreased until 17:00. Previous studies  
26 (Brown et al., 2006; Lurmann et al., 2006; Sun et al., 2012; Young et al., 2016) have attributed this  
27 type of daytime peak shortly after sunrise to the mixing-down of secondary aerosols formed at  
28 night in a residual layer aloft. Later, the photochemical formation of nitrate from  $NO_x$ , emitted  
29 from rush hour traffic, contributed to an increase in nitrate concentration during daytime, a feature  
30 of regionally generated secondary inorganic species. The decreasing trend after noon is likely due



1 to the evaporative loss of semi-volatile species at higher air temperatures as well as the dilution  
2 effects due to the enhanced BL height in the afternoon. Significant amount of nitrate can also be  
3 formed through nighttime chemistry, as indicated by the high fractional contribution during night  
4 (Fig. 5f). Given that somewhat high concentrations of O<sub>3</sub> (~12.0 ppb) and NO<sub>2</sub> (~41.7 ppb) were  
5 observed during night time (18:00 – 6:00), nitrate formation from N<sub>2</sub>O<sub>5</sub> hydrolysis possibly  
6 occurred.

7 Unlike nitrate, sulfate concentration was elevated during nighttime, showing a trend that started to  
8 increase from late afternoon (~16:00), peaked at around 10:00 on the following day, and then  
9 gradually decreased afterwards to reach a minimum value at 16:00 (Fig.5b). The overnight increase  
10 starting in the late afternoon appeared to be associated with enhanced gas-to-particle partitioning  
11 of SO<sub>2</sub> and aqueous phase processing facilitated by the relatively low temperature and high RH at  
12 night (Fig. 6). Indeed, fSO<sub>4</sub> (= the ratio in sulfate (SO<sub>4</sub><sup>2-</sup>) to SO<sub>x</sub> (SO<sub>4</sub><sup>2-</sup> + SO<sub>2</sub>) based on sulfur  
13 contents (Kaneyasu et al., 1995)) increased during night time and showed relatively good  
14 correlation with RH (R<sup>2</sup> = 0.59, Fig. 6a). However, fSO<sub>4</sub> started to decrease at ~6:00 (Fig. 6c) but  
15 sulfate concentration continued to increase till 10:00 (Fig. 6b). This increase of sulfate  
16 concentration appeared to be due to a similar reason as that of nitrate – mixing with the higher  
17 concentration of sulfate in the upper residual layer formed at night. The residual layer was also  
18 enriched of SO<sub>2</sub> (Fig. 6b), for which nighttime transport of air mass from industrial facilities  
19 located on the west and southwest outskirts of Seoul (Fig. 1b) might be responsible. However the  
20 bivariate polar plots (Fig. 7) indicate that high SO<sub>2</sub> concentration tended to occur under high speed  
21 wind from the south and southeast directions, which shifted relative to the locations of the SO<sub>2</sub>  
22 point sources (Fig. 1b). The reason might be geographical since the position (North) of the Bukhan  
23 Mountain block the wind and rather promotes the circulation of air masses. Similar trends were  
24 observed in a previous study (Heo et al., 2009).

25 The decrease of both sulfate and SO<sub>2</sub> concentrations between 10:00 and 17:00 (Fig. 6b) could to  
26 be due to the dilution effect from rising BL height. Since fSO<sub>4</sub> showed only minor increases  
27 between 12:00 and 17:00 when RH was low (Fig. 6c), gas phase photochemical production of  
28 sulfate during daytime was unlikely to be an important process. This observation, together with  
29 the nighttime increase of sulfate associated with high RH, suggests that aqueous phase processing  
30 is an important driver for sulfate formation in Seoul during wintertime. This conclusion is  
31 consistent with previous studies which found that aqueous phase reactions were an important



1 pathway for sulfate formation in the atmosphere under humid conditions (Ervens et al., 2011; Ge  
2 et al., 2012b).

3 In this study, as mentioned in the earlier section, nitrate, sulfate and chloride in PM<sub>1</sub> appeared to  
4 be fully neutralized by ammonium, indicating that the inorganic species were mainly present in  
5 the forms of NH<sub>4</sub>NO<sub>3</sub>, (NH<sub>4</sub>)<sub>2</sub>SO<sub>4</sub> and NH<sub>4</sub>Cl. Since nitrate was more abundant compared to  
6 sulfate and chloride (Fig. 4a), the ammonium diurnal pattern was similar to that of nitrate. However,  
7 a gradual increase of ammonium during nighttime was observed, likely due to the enhancement of  
8 the sulfate concentration. Chloride accounted for a small fraction of the PM<sub>1</sub> mass and displayed  
9 a morning rush hour peak, suggesting that the source of chloride is probably local, such as vehicle  
10 emissions. Indeed, the polar plot of chloride in Fig. 7 does show the feature of local source since  
11 high concentration occurred mostly at slow wind speed. Further, chloride showed a similar diurnal  
12 pattern as HOA (Section 3.3, Fig. 10) and good correlation with HOA ( $r=0.8$ ; Table 2).

13 In contrast to ammonium and nitrate, OA concentration tended to remain high overnight and  
14 started to increase in the morning with a maximum usually occurring at 8:00 (Fig. 5a). This  
15 morning increase was likely the outcome of shallow BL coupled with enhanced primary emissions  
16 from rush-hour traffic. Further discussions on this are given in section 3.3.

### 17 **3.2 Size distributions of the main components of PM<sub>1</sub>**

18 The average mass-based size distributions of AMS species in terms of vacuum aerodynamic  
19 diameter ( $D_{va}$ , (DeCarlo et al., 2004)) are shown in Fig. 4c. Nitrate and sulfate had relatively  
20 different size distribution profiles with the mode of sulfate being about 100 nm larger than the  
21 mode of nitrate. A possible reason for this difference was likely that nitrate was mainly formed  
22 through photochemical reactions whereas sulfate was more likely to be formed by aqueous-phase  
23 reactions during this study. Another reason was that sulfate was overall more aged than nitrate. As  
24 discussed in previous sections, sulfate in Seoul was likely to be transported from regional sources  
25 during nighttime whereas nitrate was apparently formed mostly locally. The daily variations in the  
26 nitrate and sulfate size distributions (Figs. 5b, c, Fig. S4) further support the different formation  
27 processes for these two compounds. The size distributions of sulfate showed a prevalent droplet  
28 accumulation mode ( $D_{va} = 500$  nm) that stayed fairly constant in concentrations and size  
29 distribution (Fig. S5b). The size distributions of nitrate stayed relatively constant throughout the  
30 day as well, but changed significantly in concentrations (Fig. S4a). In addition, nitrate size  
31 distribution was quite broad (Figs. 4c,d), similar to observations in various urban locations. (e.g.,



1 Sun et al., 2009;Sun et al., 2011a;Drewnick et al., 2004;Salcedo et al., 2006;Weimer et al.,  
2 2006;Young et al., 2016;Zhang et al., 2005b)  
3 The average size distribution of OA was wider than those of the inorganic species, peaking at a  
4  $D_{va}$  of  $\sim 400$  nm (Fig. 4c). The OA size distribution varied as a function of the time of day (Fig.  
5 5a), with a broader profile extending to  $D_{va} < 100$  nm observed during the morning rush hour and  
6 night time when primary emission are dominant. The wide size distribution of organics reflected  
7 the contribution made by both primary and secondary aerosols, i.e., the fine mode from primary  
8 aerosols and the accumulation mode from secondary formation. Similar observations were  
9 reported from China, (e.g., (Huang et al., 2010;Sun et al., 2010)) and some urban areas in North  
10 America (Aiken et al., 2009;Alfarra et al., 2004;Drewnick et al., 2004;Ge et al., 2012b;Zhang et  
11 al., 2005b) and Europe (Allan et al., 2003;Dall'Osto et al., 2013).

### 12 **3.3 OA characteristics and source apportionment**

#### 13 **3.3.1 Bulk composition and elemental ratios of OA**

14 Atmospheric OA are composed of complex materials that originate from different sources and  
15 have undergone different atmospheric processes. Understanding the chemical composition and  
16 sources of OA is important for understanding the impacts of these aerosols.

17 Overall, OA from Seoul during wintertime was found to be composed of approximately 71%  
18 carbon, 18% oxygen, 9% hydrogen, and 2% nitrogen (Fig. 4e). The average carbon-normalized  
19 molecular formula of OA was  $C_{1.8}H_{1.8}O_{0.37}N_{0.022}S_{0.0009}$ , yielding an average organic mass-to-carbon  
20 ratio (OM/OC) of 1.67. The largest component of the OA mass spectral signal was found to be the  
21  $C_xH_y^+$  ion family (57%, Fig. 4e), followed by the  $C_xH_yO_1^+$  (25%) and  $C_xH_yO_2^+$  (11%) ion families,  
22 with smaller contributions from the  $C_xH_yN_p^+$  (4%),  $C_xH_yN_pO_z^+$  (2%), and  $H_yO_1^+$  (1%) ion families.  
23 The largest peak in the average OA spectrum was at  $m/z = 43$  (Fig. 4f), accounting for 8% of the  
24 total OA signal with a composition of  $C_2H_3O^+$  (49%),  $C_3H_7^+$  (49%),  $CHON^+$  (1%), and  $C_2H_5N^+$   
25 (1%). The second largest peak (6% of the total OA signal) in the average OA spectrum was at  $m/z$   
26 = 44, which was dominated by the  $CO_2^+$  ion (86.7%) followed by  $C_2H_4O^+$  (7.8%),  $C_2H_6N^+$  (2.7%),  
27  $CH_2NO^+$  (2.6%) and  $C_3H_8^+$  (0.2%). The peak at  $m/z = 60$  was composed almost entirely of  $C_2H_4O_2^+$   
28 (94%) and 88% of the peak at  $m/z = 73$  was composed of  $C_3H_5O_2^+$ , both of which are the tracers  
29 of wood burning (Aiken et al., 2008;Alfarra et al., 2007). The peak at  $m/z = 57$ , which is used as a  
30 tracer for hydrocarbon like organics from vehicle emissions (Zhang et al., 2005a) accounted for



1 4% of the total OA signal, and was composed predominantly of  $C_4H_9^+$  (75%) and  $C_3H_5O^+$  (22%)  
2 in this study.

3 The time series of the H/C, O/C, N/C and S/C ratios of OA are shown in Figs. 3e and f. The O/C  
4 ratio of an OA indicates its average oxidation level and more aged and oxidized organics tend to  
5 have higher O/C ratios (Aiken et al., 2008; Jimenez et al., 2009). The O/C varied substantially  
6 during this study ranging from 0.05 to 0.63 and the average O/C ratio was  $0.37 \pm 0.09$ . The average  
7 H/C ratio was  $1.79 \pm 0.07$  (1.60 – 2.29) and the average OM/OC was  $1.67 \pm 0.12$  (1.26 – 2.03). These  
8 values, which were calculated using the updated elemental analysis method (Canagaratna et al.,  
9 2015), are within the range of revised values observed at other urban locations (Canagaratna et al.,  
10 2015 and references within). Upon examining the diurnal patterns, we also found that the O/C and  
11 OM/OC ratios started to increase in the morning and peaked in the afternoon (Figs. 8a and e). The  
12 lowest value of both parameters occurred at around 8:00, due to enhanced vehicle emissions during  
13 morning rush hours coupled with low BL height, which was also evident in the diurnal profile of  
14 the H/C ratio (Fig. 8b). However, during daytime (8:00 – 16:00), O/C ratio generally increased  
15 and H/C ratio decreased suggesting that SOA production or mixing with more aged aerosol from  
16 regional sources was important during daytime and outweighed the emissions POA. The decrease  
17 of the OM/OC and O/C ratios as well as the increase of H/C ratio in the late evening (19:00–  
18 20:00) were consistent with an enhancement of POA emissions during the evening rush hour and  
19 dinner time.

20 Although organic ions containing nitrogen and sulfur had relatively low abundance (average N/C  
21 = 0.018; average S/C = 0.001), both nitrogen-to-carbon (N/C) and sulfur-to-carbon (S/C) ratios  
22 showed distinct diurnal profiles where N/C enhanced during daytime (8:00 – 16:00) and increased  
23 again from late evening (19:00), suggesting that particulate nitrogen-containing compounds in  
24 Seoul were probably from both primary emissions and secondary formation. However, S/C  
25 showed relatively strong enhancement during daytime (8:00 – 16:00), suggesting that sulfur  
26 containing organics were mainly formed by secondary processes during daytime. This is further  
27 confirmed by considering the correlation between different OA factors vs. AMS spectral ions;  
28 nitrogen containing ions had good correlation both with POA and SOA factors whereas sulfur  
29 containing ions had good correlation only with OOA (Fig. S5; see section 3.3.2).

### 30 3.3.2 Organic aerosol source apportionment and characteristics of OA factors



1 Separation of distinct organic aerosol sources can be achieved through the application of  
2 multivariate models, such as PMF (Lanz et al., 2007;Ulbrich et al., 2009;Zhang et al., 2011). In  
3 this study, five OA factors were determined, consisting of three POA factors (HOA, COA and  
4 BBOA) and two SOA factors (LV-OOA and SV-OOA). The O/C ratios for the factors were: LV-  
5 OOA = 0.58; SV-OOA = 0.47; BBOA = 0.22; COA = 0.14; and HOA = 0.15. The elemental ratios  
6 of the factors were estimated using the updated method reported by Canagaratna et al. (2015). A  
7 comparison of the O/C and H/C ratio of each PMF factor, as determined by the methods of Aiken  
8 et al. (2008) and Canagaratna et al. (2015), can be found in Table S1. An overview of the chemical  
9 composition and temporal variations of the five factors is shown in Figs. 9, 10 and Fig. S7. The  
10 five factors made similar contributions to total OA mass, with LV-OOA (26%) representing the  
11 largest fraction of the OA mass and the smallest fraction accounted for by SV-OOA (15%). BBOA,  
12 COA and HOA accounted for 23, 20 and 16% of the total OA mass, respectively. Together,  
13 primary components on average accounted for 59% of the total OA mass and SOA accounted for  
14 41% (Fig. 10k). The chemical composition and temporal variations of each factor are discussed in  
15 detail below.

### 16 3.3.2.1 Hydrocarbon-like OA (HOA)

17 Alkyl fragments ( $C_nH_{2n+1}^+$  and  $C_nH_{2n-1}^+$ ) made a substantial contribution to the HOA factor, with  
18 major peaks at  $m/z$ 's 41, 43, 55, and 57 which were mostly composed of  $C_3H_5^+$ ,  $C_3H_7^+$ ,  $C_4H_7^+$ , and  
19  $C_4H_9^+$  ions, respectively (Fig. 10a). These major peaks and the overall picket fence fragmentation  
20 pattern resulting from the  $C_nH_{2n+1}^+$  ions are typical features of the HOA spectra reported in other  
21 studies and are due to the association of these aerosols with fossil fuel combustion (e.g.,Alfarra et  
22 al., 2007;Lanz et al., 2008;Sun et al., 2011b;Zhang et al., 2005a;Huang et al., 2010;Morgan et al.,  
23 2010;Ng et al., 2011). In addition, strong correlations were observed between the time series of  
24 HOA and the  $C_nH_{2n+1}^+$  and  $C_nH_{2n-1}^+$  ions, e.g.,  $C_3H_7^+$  ( $r = 0.91$ ),  $C_4H_7^+$  ( $r = 0.85$ ),  $C_4H_9^+$  ( $r = 0.95$ ),  
25 and  $C_5H_{11}^+$  ( $r = 0.96$ ) (Fig. 9a and Table 2). Due to the dominance of chemically reduced  
26 hydrocarbon species, the O/C ratio of the HOA in this study was low (0.06), whereas the H/C ratio  
27 was high (2.21). The O/C ratio of HOA of this study was similar to the updated values of HOA  
28 (0.05 – 0.25) from other studies (Canagaratna et al., 2015).

29 The regular enhancement of HOA around 7:00 – 9:00, as shown in its diurnal profile (Fig. 10f),  
30 was consistent with the occurrence of morning rush hour traffic in Seoul and the association of  
31 HOA with vehicle emissions. HOA concentration decreased rapidly from 8:00 to 12:00 noon and



1 remained low in the afternoon, mainly due to dilution associated with rising of BL height. A slow  
2 increase of HOA concentration began at ~16:00 and persisted till the next morning, suggesting  
3 that the shallow BL enhanced the gradual accumulation of the pollutants from vehicle emissions.  
4 However, the correlations of the time series of HOA with gaseous tracers of primary emissions  
5 (i.e., BC, NO<sub>2</sub>, and CO), were only moderate (Fig. 9a and Table 2), mainly because these pollutants  
6 are emitted not only from vehicular sources, but also from other combustion sources, e.g., biomass  
7 burning. Indeed, the correlations are much stronger between these pollutants and total POA (=   
8 HOA + COA + BBOA) ( $r = 0.7 - 0.81$ ; Fig. 11 and Table 2).

9 In this study, major differences were observed between weekdays and weekends for HOA  
10 including other primary species, e.g., BC and POA factors (Fig. S10). For example, the diurnal  
11 pattern of HOA and BC changed significantly between the weekdays and weekends, a general  
12 decrease in the morning rush hour peak over the weekend was observed, likely due to a decrease  
13 in commuting activities because people were more likely to be at home. This weekend effect is a  
14 typical urban features which were observed in Fresno (Young et al., 2016) and Northeastern U.S.  
15 (Zhou et al., 2016b), as well.

#### 16 3.3.2.2 Cooking OA (COA)

17 COA, as resolved by AMS OA spectra, has been widely reported in urban areas with high  
18 population densities (He et al., 2010; Huang et al., 2010; Mohr et al., 2012; Sun et al., 2011b; Young  
19 et al., 2016; Ge et al., 2012a; Wang et al., 2016; Xu et al., 2014); however no results have yet been  
20 reported from Seoul. In this study, COA was found to account for 20% of the total OA mass, higher  
21 than HOA (Fig. 10k). The diurnal pattern of COA displayed a large evening peak, with a maximum  
22 concentration occurring at 19:00, i.e., dinner time. Elevated COA concentration and larger  
23 fractional contribution to OA mass were observed throughout the night (Figs. 10g, l).

24 Similar to HOA, the mass spectrum of COA in this study also contained many alkyl fragments,  
25 but to a lesser extent (75.8 % of the total signal in COA spectrum compared to 87.9% of the total  
26 signal in HOA spectrum) (Fig. 10b). However, COA contains significantly larger amounts of  
27 oxygen-containing ions than HOA (e.g.,  $C_xH_yO_1^+ = 15.4\%$  vs. 7.6% and  $C_xH_yO_2^+ = 5.1\%$  vs. 2.3%)  
28 (Fig. 10a), and thus had a higher O/C ratio (0.14) and a lower H/C ratio (1.89). The OM/OC ratio  
29 was 1.3 and the H/C ratio is 1.78 for COA. The observed O/C ratio (0.14) of COA in Seoul was at  
30 the lower end of the range (0.14-0.27) of the revised measured O/C ratio of COA in other studies,  
31 e.g., Barcelona (0.27) (Mohr et al., 2012), New York City (NYC) (0.23) (Sun et al., 2011a) and



1 Fresno (0.14 in 2010 (Ge et al., 2012b) and 0.19 in 2013 (Young et al., 2016)). Previous studies  
2 suggest that  $C_3H_3O^+$  ( $m/z$  55) and  $C_3H_5O^+$  ( $m/z$  57) were major fragments of aliphatic acids (e.g.,  
3 linoleic acid and palmitic acid) in cooking oils or animal fat and therefore used these ions as key  
4 tracers for identifying the presence of aerosols from cooking related activities (He et al.,  
5 2004; Adhikary et al., 2010; Mohr et al., 2009; Zhao et al., 2007). In addition,  $C_5H_8O^+$  ( $m/z$  84) and  
6  $C_6H_{10}O^+$  ( $m/z$  98) have been proposed as AMS tracers for COA as well (Ge et al., 2012a; Sun et  
7 al., 2011b). In this study, the time series of COA correlated well with these ions, e.g.,  $C_3H_3O^+$  ( $r =$   
8 0.86),  $C_5H_8O^+$  ( $r = 0.93$ ),  $C_7H_{12}O^+$  ( $r = 0.89$ ), and  $C_6H_{10}O^+$  ( $r = 0.95$ ) (Fig. 9b and Table 2) and  
9 COA was a major contributor to the signals of  $C_5H_8O^+$ ,  $C_6H_{10}O^+$ , and  $C_7H_{12}O^+$ , accounting for  
10 57%, 69%, and 52%, respectively, of their signals (Fig. S6). To show the chemical difference  
11 between COA and other OA factors, Mohr et al. (2012) used the relationships between the fractions  
12 of OA signals at  $m/z$  55 and  $m/z$  57 (i.e.,  $f_{55}$  and  $f_{57}$ ) or between those of  $C_3H_3O^+$  and  $C_3H_5O^+$   
13 (i.e.,  $f_{C_3H_3O^+}$  and  $f_{C_3H_5O^+}$ ) after subtracting the contributions from the oxygenated OA factors  
14 and found that the ratios between  $m/z$  55 ( $C_4H_7^+ + C_3H_3O^+$ ) and  $m/z$  57 ( $C_4H_9^+ + C_3H_5O^+$ ) in  
15 COA were much higher (2.2 – 2.8) than the ratios (0.9–1.1) in other POAs (e.g., HOA and BBOA).  
16 The COA resolved in Seoul in this study had an  $m/z$  55 to  $m/z$  57 ratio of 2.2, within the range of  
17 the values for COA reported in Mohr et al. (2012) (Fig. S9). In addition, the ratios between  $f_{55}$   
18 and  $f_{57}$  for OA in Seoul increased proportionally as the fractional contribution of COA to total  
19 OA increased (Fig. S9b), with a “V” shape indicated by the two edges defined by the COA and  
20 the HOA factors from several urban AMS data sets (Mohr et al., 2012). These observations  
21 together confirm the identification of COA at Seoul.

### 22 3.3.2.3 Biomass burning OA (BBOA)

23 Wood combustion was found to be another important POA source (23 %, Fig. 10k) in Seoul during  
24 winter, in addition to vehicle and cooking emissions. BBOA is typically prevalent during winter  
25 in locations where wood is used for residential heating (Ge et al., 2012a; Crippa et al., 2013; Zhang  
26 et al., 2015; Young et al., 2016). The mass spectrum of BBOA showed strong signals of oxygenated  
27 ions ( $C_xH_yO_1^+$ : 27.1% of total BBOA signal and  $C_xH_yO_2^+$ : 10.6 % of total BBOA signal) and was  
28 more oxidized than HOA and COA (Fig. 10). Among the three POA factors, the O/C ratio of  
29 BBOA was the highest (0.34) and the H/C ratio was the lowest (1.74), similar to the results reported  
30 in several previous studies (e.g., Aiken et al., 2009; Ge et al., 2012a; Mohr et al., 2012). An analysis  
31 of the OA spectra (Fig. 10c) revealed the typical features of BBOA, with dominant peaks at  $m/z$



1 60 (100% being  $\text{C}_2\text{H}_4\text{O}_2^+$ ) and  $m/z$  73 (95% being  $\text{C}_3\text{H}_5\text{O}_2^+$ ), which are known fragments of  
2 levoglucosan and related species (e.g., mannosan and galactosan) (Cubison et al., 2011). Scatter  
3 plots of  $f_{44}$  versus  $f_{60}$  indicate a higher  $f_{60}$  and lower  $f_{44}$  (i.e., toward the center of the triangle  
4 area of the biomass burning plumes) as the relative importance of BBOA to the total OA increased  
5 (Fig. S9). The  $f_{44}$  and  $f_{60}$  of BBOA (0.01 vs. 0.015) in this study were also within the range of  
6 values found for the other ambient BBOA factors or biomass burning aerosols from chamber  
7 studies. HOA and COA, in contrast, had much lower  $f_{60}$  values ( $< 0.01$ ). The time series of BBOA  
8 correlated well with  $\text{C}_2\text{H}_4\text{O}_2^+$  ( $r = 0.85$ ) and  $\text{C}_3\text{H}_5\text{O}_2^+$  ( $r = 0.74$ ) (Fig. 9d and Table 2) as well as  
9 other biomass burning tracer species, including potassium ( $r = 0.63$ ) and BC ( $r = 0.82$ ). BBOA  
10 also correlated well with nitrogen-containing species, particularly  $\text{C}_3\text{H}_4\text{N}^+$  ( $r = 0.75$ ),  $\text{C}_2\text{H}_4\text{N}^+$  ( $r =$   
11  $0.70$ ) and  $\text{CHN}^+$  ( $r = 0.58$ ), which was consistent with the emissions of nitriles from biomass  
12 burning activities (Simoneit et al., 2003). There was also a strong correlation between the  
13 concentration of polycyclic aromatic hydrocarbons (PAH;  $r = 0.90$ ) and BBOA, indicating that  
14 biomass burning was a main source of PAH in Seoul during wintertime. Similarly, it was found in  
15 Fresno, California, during wintertime that BBOA correlates well with N-containing ions and PAHs  
16 (Ge et al., 2012a; Young et al., 2016). Given that PAHs are byproducts of incomplete combustion,  
17 many of which are mutagenic and carcinogenic (Dzepina et al., 2007; Hannigan et al., 1998; Marr  
18 et al., 2006), our findings suggest that adverse health effects associated with biomass burning  
19 emissions should be of concern during winter in the Seoul region.

20 BBOA was the most abundant primary OA in Seoul during this study, account for 39% of the POA  
21 mass and 23% of the total OA mass. However biomass burning is not the main fuel for the  
22 residential heating in Seoul and thus, the BBOA observed in this study must have originated from  
23 other wood burning activities, either locally or regionally. The fact that the observed BBOA was  
24 relatively oxidized ( $\text{O}/\text{C} = 0.34$ ), with a large contribution from  $m/z$  44 ( $f_{44} = 5.1\%$ ), was consistent  
25 with the observations of more aged BBOA instead of primary woodstove emissions (Crippa et al.,  
26 2013; Zhang et al., 2015; Zhou et al., 2016a). The diurnal profile of BBOA showed an enhancement  
27 at around 10:00 and a background BBOA concentration of  $\sim 1 \mu\text{g}/\text{m}^3$ . Given that the polar plot of  
28 BBOA showed high concentrations at both low and high wind speeds (Fig. 7), the sources of  
29 BBOA in Seoul likely include both local and regional wood burning activities. Local wood burning  
30 activities were possibly for the purposes of heating open and public areas (e.g., construction areas,  
31 market), dispose of leaves and woody trash in the city, and heating some residences. Regional



1 sources of BBOA are possibly from open biomass burning in agricultural area near Seoul (Heo et  
2 al., 2009) and transport from North Korea or further from Russia (Jung et al., 2016).

### 3 **3.3.2.4. Semi-volatile and low volatile oxygenated OA (SV-OOA and LV-OOA)**

4 In addition to the three POA factors, two OOA factors were identified and were found to account  
5 for an average of 41% of the OA mass (Fig. 10k). OOA is ubiquitous and dominant in the  
6 atmosphere (Jimenez et al., 2009; Zhang et al., 2007a) but usually accounts for less than half of the  
7 OA mass observed in urban locations during winter such as NYC, Tokyo, Fresno and Manchester  
8 (Zhang et al., 2007b).

9 In many cases, OOA can be further separated into a low volatile/more oxygenated OOA (LV-  
10 OOA/MO-OOA) and a semi-volatile/less oxygenated OOA (SV-OOA/LO-OOA), which represent  
11 different degrees of aging and oxidation (Jimenez et al., 2009; Ng et al., 2010, and reference  
12 therein; Setyan et al., 2012; Xu et al., 2015). In this study, two OOA factors, SV-OOA and LV-  
13 OOA were observed to account for 15 and 26% of the total OA mass, respectively (Fig. 10k). As  
14 shown in the triangle plots in Fig. S9, SV-OOA ( $O/C = 0.56$ ;  $H/C = 1.90$ ) resides within the region  
15 representing fresher SOA, with a low  $f_{44}$ , and LV-OOA ( $O/C = 0.68$ ;  $H/C = 1.61$ ) was similar to  
16 aged and highly oxidized OA, with a high  $f_{44}$ . It has been observed that fresh OOA becomes  
17 increasingly more oxidized and less volatile through aging processes in the atmosphere resulting  
18 in LV-OOA and that the evolution of SOA is regarded as a continuum of oxidation. The mass  
19 spectra of both LV-OOA and SV-OOA were very similar to the spectra of OOA factors reported  
20 in other cities (e.g., Hayes et al., 2013; Mohr et al., 2012; Zhang et al., 2014).

21 Comparisons between the time series of SV-OOA and LV-OOA factors with gaseous species ( $NO_2$ ,  
22  $CO_2$ ,  $O_3$  and  $SO_2$ ), aerosol species, and meteorological parameters further confirmed their  
23 secondary nature. As described in Table 2, SV-OOA and LV-OOA strongly correlated with nitrate  
24 ( $r = 0.87$  and  $0.63$ , respectively) and sulfate ( $r = 0.71$  and  $0.80$ , respectively), whereas the  
25 correlations between POA factors and inorganic species were low ( $r = 0.09 - 0.41$ ). The Pearson's  
26 correlation coefficient between total OOA (= SV-OOA + LV-OOA) and the sum of secondary  
27 inorganic aerosols ( $NO_3 + SO_4 + NH_4$ ) was as high as 0.91 (Fig. 11a). These results confirm the  
28 association of SV-OOA and LV-OOA with SOA.

29 As discussed above, sulfate in Seoul mainly is mainly associated with regional sources, while  
30 nitrate is often formed more locally due to the intense urban emissions of  $NO_x$ . The better  
31 correlations between SV-OOA and nitrate and between LV-OOA and sulfate (Table 2) suggest



1 that SV-OOA likely had more local sources whereas LV-OOA likely had more regional sources.  
2 Furthermore, SV-OOA correlated more strongly with methanesulfonic acid (MSA), an SOA  
3 species that tends to be semi-volatile. As shown in Table 2, the correlations of SV-OOA and LV-  
4 OOA with AMS spectral ions for MSA (Ge et al., 2012a), i.e.,  $\text{CH}_3\text{SO}_2^+$  ( $r = 0.90$  and  $0.53$ ,  
5 respectively) and  $\text{CH}_2\text{SO}_2^+$  ( $r = 0.83$  and  $0.53$ , respectively) corroborated the different natures of  
6 SV-OOA (fresher, more local) and LV-OOA (aged, more regional). The diurnal profiles of SV-  
7 OOA and LV-OOA also reflected the features of local versus regional sources (Figs. 10 i,j). SV-  
8 OOA concentration had a clear peak during mid-morning to afternoon (10:00-11:00, Fig. 10i);  
9 however, LV-OOA concentration was relatively constant throughout the day (Fig. 10j). Finally,  
10 the polar plots of both OOAs showed more dispersed features compared to the POA factors,  
11 especially HOA and COA, but SV-OOA appeared to have a stronger association with local  
12 processes, as its high concentrations tended to be associated with lower wind speed, compared to  
13 LV-OOA (Fig. 7).

#### 14 **3.4 Relative Importance of local and regional influences on air quality in Seoul** 15 **during winter**

16 In an effort to improve ambient air quality, the Korean government enacted “Special Act on  
17 Seoul Metropolitan Air Quality Improvement” to regulate the concentrations of key pollutants  
18 such as  $\text{SO}_2$ , CO,  $\text{NO}_2$ ,  $\text{O}_3$ , PM, and Pb (lead) in 2005. However, till today, Seoul is still facing  
19 poor air quality problems, especially in terms of high concentrations of  $\text{PM}_{2.5}$  and  $\text{O}_3$ .  $\text{PM}_{2.5}$  has  
20 been one of the primary concerns due to its detrimental impacts on human health as well as on  
21 visibility.  $\text{O}_3$  is an important air pollutant itself and can contribute to the secondary formation of  
22  $\text{PM}_{2.5}$ . Since the development of effective air pollution control policies must rely on knowledge  
23 about the sources, it is important to investigate the major formation processes and emission sources  
24 that contribute to the high PM loadings. Therefore, in this section, we examine how both primary  
25 emissions and secondary formation affect PM loadings in Seoul during winter.

26 Fig. 12 shows comparisons of the average concentrations of  $\text{PM}_1$  components as well as other  
27 air pollutants under high and low PM loading conditions depicted on Figs. 2 and 3. The average  
28 concentrations of all aerosol components and OA sources were 1.7 – 8.6 times higher during the  
29 high loading periods compared to the low loading periods (Table 3, Figs. 12e,f). A main reason  
30 appeared to be meteorological conditions. For example, high loading periods were generally  
31 stagnant with low wind speed ( $0.99 \pm 0.7$  m/s) (Figs. 13a,b), leading to the accumulation of



1 pollutants, especially those mainly from local sources. Indeed, among all species, SV-OOA, HOA,  
2 nitrate, and COA showed the highest increases during high loading periods and their average  
3 enhancement in concentrations were 8.6, 5.2, 4.7 and 4.5 times, respectively, of the values during  
4 the low loading periods (Fig. 12e). In addition to accumulate primary pollutants, stable  
5 meteorology condition can also lead to longer atmospheric residence time, which facilitates the  
6 local formation of secondary species such as SV-OOA and nitrate. Furthermore, the relatively high  
7 RH during the high loading periods ( $71\% \pm 15$ ; Table 3, Fig. 12a) likely also enhanced the  
8 formation of secondary species such as sulfate and LV-OOA through aqueous-phase processing.  
9 A further evidence for enhanced aqueous-phase processing of secondary aerosol species during  
10 high PM loading periods is shown in Fig. 13; the size distributions of all secondary inorganic  
11 species (nitrate, sulfate and ammonium) were significantly larger during the more polluted periods,  
12 peaking at 500-600 nm in  $D_{va}$ , compared to the cleaner periods (peaking at 300-400 nm). A  
13 previous study in a US city during winter time also observed that high RH conditions, thus  
14 enhanced aqueous-phase processing, led to increases in the size modes of sulfate, nitrate, and  
15 ammonium (Ge et al., 2012b).

16 The enhancement ratios of the other primary pollutants such as CO, SO<sub>2</sub>, NO<sub>2</sub>, BC, and BBOA,  
17 were in the range of 1.2 – 2.5, significantly lower than those of HOA and COA (Fig. 12e),  
18 reflecting the facts that they all had bigger contributions from regional sources compared to HOA  
19 and COA (Fig. 7). Average O<sub>3</sub> concentration, on the other hand, showed a substantial decrease (by  
20 ~ 70%) during high aerosol loading periods (Fig. 12e and 12f). In addition to enhanced titration  
21 reactions by NO<sub>x</sub>, another possible reason was reduced photochemical reactions due to inhibition  
22 of light by high concentration of PM (He et al., 2014).

23 The high loading periods corresponded closely to air masses that are classified as cluster 4 (Fig.  
24 14), which had the shorted trajectories, i.e., slowest wind speeds, as well as the lowest travel height  
25 compared to the other three clusters. The air mass in cluster 4 thus likely held larger amounts of  
26 pollutants and precursors from the ground. In addition, PM in this type of air masses could also be  
27 more oxidized, containing a larger fraction of secondary pollutants, due to longer residence time  
28 in the atmosphere, therefore was composed of a higher fraction of nitrate.

29 The average aerosol composition during the high loading periods (Fig. 12) was similar to that  
30 for the whole period (Fig. 4), consistent with frequent occurrence of high aerosol pollution  
31 episodes and indicate that these events determined the overall characteristics of PM<sub>1</sub> in Seoul



1 during winter. Given that local emissions were mostly responsible for these pollution events,  
2 controlling the emissions of both primary aerosol particles and precursors for secondary species  
3 from local sources might be an effective way to manage air quality in Seoul during winter time.

4 Low PM loading periods (average  $\pm 1\sigma = 12.6 \pm 7.1 \mu\text{g m}^{-3}$  for  $\text{PM}_{10}$ ) were commonly  
5 associated with high WS ( $1.8 \pm 1.1 \text{ m/s}$ ), low RH (50 %), and long distance transport of air masses  
6 from northern China (such as Inner Mongolia), Mongolia or North Korea (i.e., Cluster 1, 2 and 3  
7 from backtrajectory analysis; Fig. 14). Aerosol composition was somewhat different between high  
8 loading and low loading periods. Since strong wind could inhibit the accumulation of local primary  
9 and secondary species while bring in pollutants from upwind sources, the mass fractions of species  
10 influenced by local sources, such as nitrate, SV-OOA, HOA, and COA were lower, whereas those  
11 of regional sources such as sulfate, LV-OOA, BBOA enhanced during low loading periods  
12 compared to more polluted periods (Fig. 12). Although Clusters 1, 2 and 3 all represented regional  
13 transport conditions, PM mass concentrations and compositions were somewhat different because  
14 of different origin of air masses. Specifically, Cluster 1 and 2 were almost directly to the north  
15 whereas Cluster 3 was more towards the west (Fig. 14). In comparison, Cluster 1 and 2 had higher  
16 fractions of BBOA but a lower fraction of LV-OOA and sulfate. A possible explanation for this  
17 observation is that northwest area might have more anthropogenic sources than the north area does.

18 As shown in Fig. 2, PM concentration often changed abruptly with the appearance and  
19 dissipation of a high  $\text{PM}_{10}$  event occurring rather quickly (within several hours). The changes were  
20 commonly associated with changes in meteorological conditions, especially wind direction and  
21 speed. Similar trends of sudden changes in air quality have also been observed in other studies in  
22 China, and have been attributed to meteorology (Zhang et al., 2015). For these reasons, it appears  
23 that regional meteorology played an important role in causing high PM pollution conditions in  
24 Seoul.

25

#### 26 **4 Conclusions**

27 Aerosol composition, size distribution, sources, and evolution processes were investigated using  
28 an HR-ToF-AMS and an SMPS in Seoul, Korea, during winter 2015. The average  $\text{PM}_{10}$   
29 concentration was  $27.5 \mu\text{g m}^{-3}$  and the total mass was dominated by organics (44%), followed by  
30 nitrate (24%) and sulfate (10%). Secondary materials (i.e.,  $\text{NO}_3^-$ ,  $\text{SO}_4^{2-}$ ,  $\text{NH}_4^+$ , SV-OOA and LV-  
31 OOA) together accounted for 64% of the  $\text{PM}_{10}$  total mass, with the remainder being primary



1 materials (HOA, COA, BBOA and BC). Cooking, fossil fuel combustion, and wood combustion  
2 were identified as major POA sources in Seoul, contributing an average 59% of total OA mass  
3 during this study.

4 Meteorological conditions and various emission sources influenced the concentrations,  
5 compositions, size distributions, and properties of aerosol particles in Seoul. High PM pollution  
6 periods tended to build up over a period of 4-5 days and were interleaved with multiple days of  
7 relatively clean periods. High aerosol loading periods were commonly found under relatively  
8 stagnant conditions with low wind speed and aerosol from these periods was characterized with  
9 enhanced fractional contributions of nitrate (27%) and SV-OOA (8%), indicating a strong  
10 influence from local production of secondary aerosol. In contrast, under relatively dynamic  
11 meteorological conditions with higher wind speed, aerosol loading was generally low and PM<sub>1</sub>  
12 contained larger fractions of species with regional sources, such as sulfate (12%), LV-OOA (20%),  
13 and BBOA (12%). The average O/C ratio of OA was also higher during low loading periods (0.41  
14 vs. 0.35 for high loading periods), indicating the influence of more oxidized OA likely from long  
15 range transport.

16 Total POA concentration was enhanced by three times during high loading periods. In addition,  
17 enhanced fractional contribution of BBOA was observed during low loading period. In this study,  
18 we found that nearly half of the OA mass was POA and that PAHs in PM<sub>1</sub> were mainly from  
19 biomass burning and vehicle emission sources. These results suggest that it is important to reduce  
20 emissions from combustion sources to improve air quality and protect public health in Seoul during  
21 wintertime. Together, local formation of secondary species (e.g., Nitrate, SV-OOA) during stable  
22 meteorological conditions was also significant for high PM loadings. Thus, the serious pollution  
23 observed in Seoul during winter was caused by combination of factors, including meteorological  
24 conditions, emission by local primary sources, secondary formation as well as transport of air  
25 masses from upwind locations and other unknown factors.

26

## 27 **Acknowledgments**

28 This work was supported by the Korea Institute of Science and Technology (KIST). QZ  
29 acknowledges the Changjiang Scholars program of the Chinese Ministry of Education.

30

31



## 1 References

- 2 Adhikary, B., Carmichael, G. R., Kulkarni, S., Wei, C., Tang, Y., D'Allura, A., Mena-Carrasco, M., Streets,  
3 D. G., Zhang, Q., Pierce, R. B., Al-Saadi, J. A., Emmons, L. K., Pfister, G. G., Avery, M. A., Barrick,  
4 J. D., Blake, D. R., Brune, W. H., Cohen, R. C., Dibb, J. E., Fried, A., Heikes, B. G., Huey, L. G.,  
5 O'Sullivan, D. W., Sachse, G. W., Shetter, R. E., Singh, H. B., Campos, T. L., Cantrell, C. A., Flocke,  
6 F. M., Dunlea, E. J., Jimenez, J. L., Weinheimer, A. J., Crouse, J. D., Wennberg, P. O., Schauer, J. J.,  
7 Stone, E. A., Jaffe, D. A., and Reidmiller, D. R.: A regional scale modeling analysis of aerosol and  
8 trace gas distributions over the eastern Pacific during the INTEX-B field campaign, *Atmospheric  
9 Chemistry and Physics*, 10, 2091-2115, 2010.
- 10 Aiken, A. C., Decarlo, P. F., Kroll, J. H., Worsnop, D. R., Huffman, J. A., Docherty, K. S., Ulbrich, I. M.,  
11 Mohr, C., Kimmel, J. R., Sueper, D., Sun, Y., Zhang, Q., Trimborn, A., Northway, M., Ziemann, P. J.,  
12 Canagaratna, M. R., Onasch, T. B., Alfarra, M. R., Prevot, A. S. H., Dommen, J., Duplissy, J., Metzger,  
13 A., Baltensperger, U., and Jimenez, J. L.: O/C and OM/OC ratios of primary, secondary, and ambient  
14 organic aerosols with high-resolution time-of-flight aerosol mass spectrometry, *Environmental Science  
15 & Technology*, 42, 4478-4485, 10.1021/es703009q, 2008.
- 16 Aiken, A. C., Salcedo, D., Cubison, M. J., Huffman, J. A., DeCarlo, P. F., Ulbrich, I. M., Docherty, K. S.,  
17 Sueper, D., Kimmel, J. R., Worsnop, D. R., Trimborn, A., Northway, M., Stone, E. A., Schauer, J. J.,  
18 Volkamer, R. M., Fortner, E., de Foy, B., Wang, J., Laskin, A., Shutthanandan, V., Zheng, J., Zhang,  
19 R., Gaffney, J., Marley, N. A., Paredes-Miranda, G., Arnott, W. P., Molina, L. T., Sosa, G., and  
20 Jimenez, J. L.: Mexico City aerosol analysis during MILAGRO using high resolution aerosol mass  
21 spectrometry at the urban supersite (T0) – Part 1: Fine particle composition and organic source  
22 apportionment, *Atmospheric Chemistry and Physics*, 9, 6633-6653, 10.5194/acp-9-6633-2009, 2009.
- 23 Alfarra, M. R., Coe, H., Allan, J. D., Bower, K. N., Boudries, H., Canagaratna, M. R., Jimenez, J. L., Jayne,  
24 J. T., Garforth, A., Li, S.-M., and Worsnop, D. R.: Characterization of urban and rural organic  
25 particulate in the Lower Fraser Valley using two Aerodyne Aerosol Mass Spectrometers, *Atmospheric  
26 Environment*, 38, 13, 2004.
- 27 Alfarra, M. R., Prevot, A. S. H., Szidat, S., Sandradewi, J., Weimer, S., Lanz, V. A., Schreiber, D., Mohr,  
28 M., and Baltensperger, U.: Identification of the Mass Spectral Signature of Organic Aerosols from  
29 Wood Burning Emissions, *Environmental Science & Technology*, 41, 5770-5777, 10.1021/es062289b,  
30 2007.
- 31 Allan, J. D., Alfarra, M. R., Bower, K. N., Williams, P. I., Gallagher, M. W., Jimenez, J. L., McDonald, A.  
32 G., Nemitz, E., Canagaratna, M. R., Jayne, J. T., Coe, H., and Worsnop, D. R.: Quantitative sampling  
33 using an Aerodyne aerosol mass spectrometer - 2. Measurements of fine particulate chemical  
34 composition in two U.K. cities, *Journal of Geophysical Research-Atmospheres*, 108,  
35 10.1029/2002jd002359, 2003.
- 36 Allan, J. D., Delia, A. E., Coe, H., Bower, K. N., Alfarra, M. R., Jimenez, J. L., Middlebrook, A. M.,  
37 Drewnick, F., Onasch, T. B., Canagaratna, M. R., Jayne, J. T., and Worsnop, D. R.: A generalised  
38 method for the extraction of chemically resolved mass spectra from aerodyne aerosol mass  
39 spectrometer data, *J Aerosol Sci*, 35, 909-922, 10.1016/j.jaerosci.2004.02.007, 2004.
- 40 Brown, S. G., Roberts, P. T., McCarthy, M. C., Lurmann, F. W., and Hyslop, N. P.: Wintertime vertical  
41 variations in particulate matter (PM) and precursor concentrations in the San Joaquin Valley during the  
42 California Regional coarse PM/fine PM Air Quality Study, *Journal of the Air & Waste Management  
43 Association*, 56, 1267-1277, 2006.
- 44 Canagaratna, M. R., Jayne, J. T., Jimenez, J. L., Allan, J. D., Alfarra, M. R., Zhang, Q., Onasch, T. B.,  
45 Drewnick, F., Coe, H., Middlebrook, A., Delia, A., Williams, L. R., Trimborn, A. M., Northway, M.  
46 J., DeCarlo, P. F., Kolb, C. E., Davidovits, P., and Worsnop, D. R.: Chemical and microphysical



- 1 characterization of ambient aerosols with the aerodyne aerosol mass spectrometer, *Mass Spectrometry*  
2 *Reviews*, 26, 185-222, 10.1002/mas.20115, 2007.
- 3 Canagaratna, M. R., Jimenez, J. L., Kroll, J. H., Chen, Q., Kessler, S. H., Massoli, P., Hildebrandt Ruiz, L.,  
4 Fortner, E., Williams, L. R., Wilson, K. R., Surratt, J. D., Donahue, N. M., Jayne, J. T., and Worsnop,  
5 D. R.: Elemental ratio measurements of organic compounds using aerosol mass spectrometry:  
6 characterization, improved calibration, and implications, *Atmospheric Chemistry and Physics*, 15, 253-  
7 272, 10.5194/acp-15-253-2015, 2015.
- 8 Cao, J.-j., Wang, Q.-y., Chow, J. C., Watson, J. G., Tie, X.-x., Shen, Z.-x., Wang, P., and An, Z.-s.: Impacts  
9 of aerosol compositions on visibility impairment in Xi'an, China, *Atmospheric Environment*, 59, 559-  
10 566, 10.1016/j.atmosenv.2012.05.036, 2012.
- 11 Choi, J.-K., Heo, J.-B., Ban, S.-J., Yi, S.-M., and Zoh, K.-D.: Chemical characteristics of PM<sub>2.5</sub> aerosol in  
12 Incheon, Korea, *Atmospheric Environment*, 60, 583-592, 2012.
- 13 Choi, N. R., Lee, S. P., Lee, J. Y., Jung, C. H., and Kim, Y. P.: Speciation and source identification of  
14 organic compounds in PM<sub>10</sub> over Seoul, South Korea, *Chemosphere*, 144, 1589-1596,  
15 10.1016/j.chemosphere.2015.10.041, 2016.
- 16 Crippa, M., DeCarlo, P. F., Slowik, J. G., Mohr, C., Heringa, M. F., Chirico, R., Poulain, L., Freutel, F.,  
17 Sciare, J., Cozic, J., Di Marco, C. F., Elsasser, M., Nicolas, J. B., Marchand, N., Abidi, E.,  
18 Wiedensohler, A., Drewnick, F., Schneider, J., Borrmann, S., Nemitz, E., Zimmermann, R., Jaffrezo,  
19 J. L., Prevot, A. S. H., and Baltensperger, U.: Wintertime aerosol chemical composition and source  
20 apportionment of the organic fraction in the metropolitan area of Paris, *Atmospheric Chemistry and*  
21 *Physics*, 13, 961-981, 10.5194/acp-13-961-2013, 2013.
- 22 Cubison, M. J., Ortega, A. M., Hayes, P. L., Farmer, D. K., Day, D., Lechner, M. J., Brune, W. H., Apel,  
23 E., Diskin, G. S., Fisher, J. A., Fuelberg, H. E., Hecobian, A., Knapp, D. J., Mikoviny, T., Riemer, D.,  
24 Sachse, G. W., Sessions, W., Weber, R. J., Weinheimer, A. J., Wisthaler, A., and Jimenez, J. L.: Effects  
25 of aging on organic aerosol from open biomass burning smoke in aircraft and laboratory studies,  
26 *Atmospheric Chemistry and Physics*, 11, 12049-12064, 10.5194/acp-11-12049-2011, 2011.
- 27 Dall'Osto, M., Ovadnevaite, J., Ceburnis, D., Martin, D., Healy, R. M., O'Connor, I. P., Kourchev, I.,  
28 Sodeau, J. R., Wenger, J. C., and O'Dowd, C.: Characterization of urban aerosol in Cork city (Ireland)  
29 using aerosol mass spectrometry, *Atmospheric Chemistry and Physics*, 13, 4997-5015, 10.5194/acp-  
30 13-4997-2013, 2013.
- 31 DeCarlo, P. F., Slowik, J. G., Worsnop, D. R., Davidovits, P., and Jimenez, J. L.: Particle morphology and  
32 density characterization by combined mobility and aerodynamic diameter measurements. Part 1:  
33 Theory, *Aerosol Science and Technology*, 38, 1185-1205, Doi 10.1080/02786820590928897, 2004.
- 34 DeCarlo, P. F., Kimmel, J. R., Trimborn, A., Northway, M. J., Jayne, J. T., Aiken, A. C., Gonin, M., Fuhrer,  
35 K., Horvath, T., Docherty, K. S., Worsnop, D. R., and Jimenez, J. L.: Field-deployable, high-resolution,  
36 time-of-flight aerosol mass spectrometer, *Analytical Chemistry*, 78, 8281-8289, 10.1021/ac061249n,  
37 2006.
- 38 Ding, A. J., Fu, C. B., Yang, X. Q., Sun, J. N., Zheng, L. F., Xie, Y. N., Herrmann, E., Nie, W., Petaja, T.,  
39 Kerminen, V. M., and Kulmala, M.: Ozone and fine particle in the western Yangtze River Delta: an  
40 overview of 1 yr data at the SORPES station, *Atmospheric Chemistry and Physics*, 13, 5813-5830,  
41 10.5194/acp-13-5813-2013, 2013.
- 42 Ding, A. J., Huang, X., Nie, W., Sun, J. N., Kerminen, V. M., Petäjä, T., Su, H., Cheng, Y. F., Yang, X. Q.,  
43 Wang, M. H., Chi, X. G., Wang, J. P., Virkkula, A., Guo, W. D., Yuan, J., Wang, S. Y., Zhang, R. J.,  
44 Wu, Y. F., Song, Y., Zhu, T., Zilitinkevich, S., Kulmala, M., and Fu, C. B.: Enhanced haze pollution  
45 by black carbon in megacities in China, *Geophysical Research Letters*, 43, 2873-2879,  
46 10.1002/2016gl067745, 2016.



- 1 Draxler, R. R., Stunder, B., Rolph, G., Stein, A., and Taylor, A.: HYSPLIT\_4 User's Guide, available at  
2 [http://www.arl.noaa.gov/documents/reports/hysplit\\_user\\_guide.pdf](http://www.arl.noaa.gov/documents/reports/hysplit_user_guide.pdf), NOAA Air Resources Laboratory,  
3 Silver Spring, Maryland, USA  
4 2012.
- 5 Draxler, R. R. a. H., G. D.: Description of the HYSPLIT\_4 modeling system, available at:  
6 <http://www.arl.noaa.gov/documents/reports/arl-224.pdf> (last access: 5 January 2014), NOAA Air  
7 Resources Laboratory, Silver Spring, Maryland, USA, 1997.
- 8 Drewnick, F., Jayne, J. T., Canagaratna, M., Worsnop, D. R., and Demerjian, K. L.: Measurement of  
9 ambient aerosol composition during the PMTACS-NY 2001 using an aerosol mass spectrometer. Part  
10 II: Chemically speciated mass distributions, *Aerosol Science and Technology*, 38, 104-117,  
11 10.1080/02786820390229534, 2004.
- 12 Dzepina, K., Arey, J., Marr, L. C., Worsnop, D. R., Salcedo, D., Zhang, Q., Onasch, T. B., Molina, L. T.,  
13 Molina, M. J., and Jimenez, J. L.: Detection of particle-phase polycyclic aromatic hydrocarbons in  
14 Mexico City using an aerosol mass spectrometer, *Int J Mass Spectrom*, 263, 152-170,  
15 <http://dx.doi.org/10.1016/j.ijms.2007.01.010>, 2007.
- 16 Ervens, B., Turpin, B. J., and Weber, R. J.: Secondary organic aerosol formation in cloud droplets and  
17 aqueous particles (aqSOA): a review of laboratory, field and model studies, *Atmospheric Chemistry  
18 and Physics*, 11, 11069-11102, 10.5194/acp-11-11069-2011, 2011.
- 19 Ge, X., Setyan, A., Sun, Y., and Zhang, Q.: Primary and secondary organic aerosols in Fresno, California  
20 during wintertime: Results from high resolution aerosol mass spectrometry, *Journal of Geophysical  
21 Research-Atmospheres*, 117, 10.1029/2012jd018026, 2012a.
- 22 Ge, X. L., Zhang, Q., Sun, Y. L., Ruehl, C. R., and Setyan, A.: Effect of aqueous-phase processing on  
23 aerosol chemistry and size distributions in Fresno, California, during wintertime, *Environ. Chem.*, 9,  
24 221-235, 10.1071/en11168, 2012b.
- 25 Gelencsér, A., May, B., Simpson, D., Sánchez-Ochoa, A., Kasper-Giebl, A., Puxbaum, H., Caseiro, A., Pio,  
26 C., and Legrand, M.: Source apportionment of PM<sub>2.5</sub> organic aerosol over Europe: Primary/secondary,  
27 natural/anthropogenic, and fossil/biogenic origin, - 112, 2007.
- 28 Guo, S., Hu, M., Zamora, M. L., Peng, J., Shang, D., Zheng, J., Du, Z., Wu, Z., Shao, M., Zeng, L., Molina,  
29 M. J., and Zhang, R.: Elucidating severe urban haze formation in China, *Proceedings of the National  
30 Academy of Sciences*, 111, 17373-17378, 10.1073/pnas.1419604111, 2014.
- 31 Hannigan, M. P., Cass, G. R., Penman, B. W., Crespi, C. L., Lafleur, A. L., Busby, W. F., Thilly, W. G.,  
32 and Simoneit, B. R. T.: Bioassay-Directed Chemical Analysis of Los Angeles Airborne Particulate  
33 Matter Using a Human Cell Mutagenicity Assay, *Environ Sci Technol*, 32, 3502-3514,  
34 10.1021/es9706561, 1998.
- 35 Harrison, R. M., and Yin, J.: Particulate matter in the atmosphere: which particle properties are important  
36 for its effects on health?, *Science of the Total Environment*, 249, 85-101,  
37 [http://dx.doi.org/10.1016/S0048-9697\(99\)00513-6](http://dx.doi.org/10.1016/S0048-9697(99)00513-6), 2000.
- 38 Hayes, P. L., Ortega, A. M., Cubison, M. J., Froyd, K. D., Zhao, Y., Cliff, S. S., Hu, W. W., Toohey, D.  
39 W., Flynn, J. H., Lefer, B. L., Grossberg, N., Alvarez, S., Rappenglueck, B., Taylor, J. W., Allan, J. D.,  
40 Holloway, J. S., Gilman, J. B., Kuster, W. C., De Gouw, J. A., Massoli, P., Zhang, X., Liu, J., Weber,  
41 R. J., Corrigan, A. L., Russell, L. M., Isaacman, G., Worton, D. R., Kreisberg, N. M., Goldstein, A. H.,  
42 Thalman, R., Waxman, E. M., Volkamer, R., Lin, Y. H., Surratt, J. D., Kleindienst, T. E., Offenberg,  
43 J. H., Dusanter, S., Griffith, S., Stevens, P. S., Brioude, J., Angevine, W. M., and Jimenez, J. L.: Organic  
44 aerosol composition and sources in Pasadena, California, during the 2010 CalNex campaign, *Journal  
45 of Geophysical Research-Atmospheres*, 118, 9233-9257, 10.1002/jgrd.50530, 2013.



- 1 He, H., Wang, Y. S., Ma, Q. X., Ma, J. Z., Chu, B. W., Ji, D. S., Tang, G. Q., Liu, C., Zhang, H. X., and  
2 Hao, J. M.: Mineral dust and NO<sub>x</sub> promote the conversion of SO<sub>2</sub> to sulfate in heavy pollution days,  
3 *Scientific Reports*, 4, 10.1038/srep04172, 2014.
- 4 He, J., Zielinska, B., and Balasubramanian, R.: Composition of semi-volatile organic compounds in the  
5 urban atmosphere of Singapore: influence of biomass burning, *Atmospheric Chemistry and Physics*,  
6 10, 11401-11413, 10.5194/acp-10-11401-2010, 2010.
- 7 He, L.-Y., Huang, X.-F., Xue, L., Hu, M., Lin, Y., Zheng, J., Zhang, R., and Zhang, Y.-H.: Submicron  
8 aerosol analysis and organic source apportionment in an urban atmosphere in Pearl River Delta of China  
9 using high-resolution aerosol mass spectrometry, *Journal of Geophysical Research-Atmospheres*, 116,  
10 10.1029/2010jd014566, 2011.
- 11 He, L. Y., Hu, M., Huang, X. F., Yu, B. D., Zhang, Y. H., and Liu, D. Q.: Measurement of emissions of  
12 fine particulate organic matter from Chinese cooking, *Atmospheric Environment*, 38, 6557-6564,  
13 10.1016/j.atmosenv.2004.08.034, 2004.
- 14 Heo, J. B., Hopke, P. K., and Yi, S. M.: Source apportionment of PM<sub>2.5</sub> in Seoul, Korea, *Atmospheric  
15 Chemistry and Physics*, 9, 4957-4971, 2009.
- 16 Huang, R.-J., Zhang, Y., Bozzetti, C., Ho, K.-F., Cao, J.-J., Han, Y., Daellenbach, K. R., Slowik, J. G.,  
17 Platt, S. M., Canonaco, F., Zotter, P., Wolf, R., Pieber, S. M., Bruns, E. A., Crippa, M., Ciarelli, G.,  
18 Piazzalunga, A., Schwikowski, M., Abbaszade, G., Schnelle-Kreis, J., Zimmermann, R., An, Z., Szidat,  
19 S., Baltensperger, U., El Haddad, I., and Prevot, A. S. H.: High secondary aerosol contribution to  
20 particulate pollution during haze events in China, *Nature*, 514, 218-222, 10.1038/nature13774, 2014.
- 21 Huang, X. F., He, L. Y., Hu, M., Canagaratna, M. R., Sun, Y., Zhang, Q., Zhu, T., Xue, L., Zeng, L. W.,  
22 Liu, X. G., Zhang, Y. H., Jayne, J. T., Ng, N. L., and Worsnop, D. R.: Highly time-resolved chemical  
23 characterization of atmospheric submicron particles during 2008 Beijing Olympic Games using an  
24 Aerodyne High-Resolution Aerosol Mass Spectrometer, *Atmospheric Chemistry and Physics*, 10,  
25 8933-8945, 10.5194/acp-10-8933-2010, 2010.
- 26 Huang, X. F., He, L. Y., Hu, M., Canagaratna, M. R., Kroll, J. H., Ng, N. L., Zhang, Y. H., Lin, Y., Xue,  
27 L., Sun, T. L., Liu, X. G., Shao, M., Jayne, J. T., and Worsnop, D. R.: Characterization of submicron  
28 aerosols at a rural site in Pearl River Delta of China using an Aerodyne High-Resolution Aerosol Mass  
29 Spectrometer, *Atmospheric Chemistry and Physics*, 11, 1865-1877, 10.5194/acp-11-1865-2011, 2011.
- 30 Huang, X. F., He, L. Y., Xue, L., Sun, T. L., Zeng, L. W., Gong, Z. H., Hu, M., and Zhu, T.: Highly time-  
31 resolved chemical characterization of atmospheric fine particles during 2010 Shanghai World Expo,  
32 *Atmospheric Chemistry and Physics*, 12, 4897-4907, 10.5194/acp-12-4897-2012, 2012.
- 33 IPCC: Summary for policymakers, in: *Climate Change 2013: The Physical Science Basis. Contribution of  
34 Working Group I to the Fifth Assessment Report of the Intergovernmental Panel on Climate Change*,  
35 edited by: Stocker, T. F., Qin, D., Plattner, G.-K., Tignor, M., Allen, S. K., Boschung, J., Nauels, A.,  
36 Xia, Y., Bex, V., and Midgley, P. M., Cambridge University Press, Cambridge, UK, New York, NY,  
37 USA, 3-29, 2013.
- 38 Jimenez, J. L., Canagaratna, M. R., Donahue, N. M., Prevot, A. S. H., Zhang, Q., Kroll, J. H., DeCarlo, P.  
39 F., Allan, J. D., Coe, H., Ng, N. L., Aiken, A. C., Docherty, K. S., Ulbrich, I. M., Grieshop, A. P.,  
40 Robinson, A. L., Duplissy, J., Smith, J. D., Wilson, K. R., Lanz, V. A., Hueglin, C., Sun, Y. L., Tian,  
41 J., Laaksonen, A., Raatikainen, T., Rautiainen, J., Vaattovaara, P., Ehn, M., Kulmala, M., Tomlinson,  
42 J. M., Collins, D. R., Cubison, M. J., Dunlea, E. J., Huffman, J. A., Onasch, T. B., Alfarra, M. R.,  
43 Williams, P. I., Bower, K., Kondo, Y., Schneider, J., Drewnick, F., Borrmann, S., Weimer, S.,  
44 Demerjian, K., Salcedo, D., Cottrell, L., Griffin, R., Takami, A., Miyoshi, T., Hatakeyama, S.,  
45 Shimono, A., Sun, J. Y., Zhang, Y. M., Dzepina, K., Kimmel, J. R., Sueper, D., Jayne, J. T., Herndon,  
46 S. C., Trimborn, A. M., Williams, L. R., Wood, E. C., Middlebrook, A. M., Kolb, C. E., Baltensperger,



- 1 U., and Worsnop, D. R.: Evolution of Organic Aerosols in the Atmosphere, *Science*, 326, 1525-1529,  
2 10.1126/science.1180353, 2009.
- 3 Jung, J., Lyu, Y., Lee, M., Hwang, T., Lee, S., and Oh, S.: Impact of Siberian forest fires on the atmosphere  
4 over the Korean Peninsula during summer 2014, *Atmospheric Chemistry and Physics*, 16, 6757-6770,  
5 10.5194/acp-16-6757-2016, 2016.
- 6 Kaneyasu, N., Ohta, S., and Murao, N.: SEASONAL-VARIATION IN THE CHEMICAL-  
7 COMPOSITION OF ATMOSPHERIC AEROSOLS AND GASEOUS SPECIES IN SAPPORO,  
8 JAPAN, *Atmospheric Environment*, 29, 1559-1568, 10.1016/1352-2310(94)00356-p, 1995.
- 9 Kang, S. H., Heo, J., Oh, I. Y., Kim, J., Lim, W. H., Cho, Y., Choi, E. K., Yi, S. M., Do Shin, S., Kim, H.,  
10 and Oh, S.: Ambient air pollution and out-of-hospital cardiac arrest, *Int. J. Cardiol.*, 203, 1086-1092,  
11 10.1016/j.ijcard.2015.11.100, 2016.
- 12 Kim, E., Hopke, P. K., and Edgerton, E. S.: Source identification of Atlanta aerosol by positive matrix  
13 factorization, *Journal of the Air & Waste Management Association*, 53, 731-739, 2003.
- 14 Kim, Y., Yoon, S. C., Kim, S. W., Kim, K. Y., Lim, H. C., and Ryu, J.: Observation of new particle  
15 formation and growth events in Asian continental outflow, *Atmospheric Environment*, 64, 160-168,  
16 10.1016/j.atmosenv.2012.09.057, 2013.
- 17 Kim, Y., Kim, S.-W., Yoon, S.-C., Kim, M.-H., and Park, K.-H.: Aerosol properties and associated regional  
18 meteorology during winter pollution event at Gosan climate observatory, Korea, *Atmospheric  
19 Environment*, 85, 9-17, 10.1016/j.atmosenv.2013.11.041, 2014.
- 20 KOSAE: Studies of Measures for Improving/Complementing the Master Plan for the Metropolitan Air  
21 Quality Management. Report to the Korean Ministry of Environment (in Korean), Gwacheon, Korea. ,  
22 2009.
- 23 Kulmala, M., Lappalainen, H. K., Petaja, T., Kurten, T., Kerminen, V. M., Viisanen, Y., Hari, P., Sorvari,  
24 S., Back, J., Bondur, V., Kasimov, N., Kotlyakov, V., Matvienko, G., Baklanov, A., Guo, H. D., Ding,  
25 A., Hansson, H. C., and Zilitinkevich, S.: Introduction: The Pan-Eurasian Experiment (PEEX) -  
26 multidisciplinary, multiscale and multicomponent research and capacity-building initiative,  
27 *Atmospheric Chemistry and Physics*, 15, 13085-13096, 10.5194/acp-15-13085-2015, 2015.
- 28 Kuwata, M., Zorn, S. R., and Martin, S. T.: Using Elemental Ratios to Predict the Density of Organic  
29 Material Composed of Carbon, Hydrogen, and Oxygen, *Environmental Science & Technology*, 46,  
30 787-794, 10.1021/es202525q, 2012.
- 31 Lanz, V. A., Alfarra, M. R., Baltensperger, U., Buchmann, B., Hueglin, C., and Prevot, A. S. H.: Source  
32 apportionment of submicron organic aerosols at an urban site by factor analytical modelling of aerosol  
33 mass spectra, *Atmospheric Chemistry and Physics*, 7, 1503-1522, 2007.
- 34 Lanz, V. A., Alfarra, M. R., Baltensperger, U., Buchmann, B., Hueglin, C., Szidat, S., Wehrli, M. N.,  
35 Wacker, L., Weimer, S., Caseiro, A., Puxbaum, H., and Prevot, A. S. H.: Source Attribution of Aerosol  
36 Submicron Organic Aerosols during Wintertime Inversions by Advanced Factor Analysis of Aerosol  
37 Mass Spectra, *Environmental Science & Technology*, 42, 214-220, 10.1021/es0707207, 2008.
- 38 Li, Y. J., Lee, B. P., Su, L., Fung, J. C. H., and Chan, C. K.: Seasonal characteristics of fine particulate  
39 matter (PM) based on high-resolution time-of-flight aerosol mass spectrometric (HR-ToF-AMS)  
40 measurements at the HKUST Supersite in Hong Kong, *Atmos. Chem. Phys.*, 15, 37-53, 10.5194/acp-  
41 15-37-2015, 2015.
- 42 Lim, S., Lee, M., Lee, G., Kim, S., Yoon, S., and Kang, K.: Ionic and carbonaceous compositions of PM10,  
43 PM2.5 and PM1.0 at Gosan ABC Superstation and their ratios as source signature, *Atmospheric  
44 Chemistry and Physics*, 12, 2007-2024, 10.5194/acp-12-2007-2012, 2012.



- 1 Liu, X. G., Li, J., Qu, Y., Han, T., Hou, L., Gu, J., Chen, C., Yang, Y., Liu, X., Yang, T., Zhang, Y., Tian,  
2 H., and Hu, M.: Formation and evolution mechanism of regional haze: a case study in the megacity  
3 Beijing, China, *Atmospheric Chemistry and Physics*, 13, 4501-4514, 10.5194/acp-13-4501-2013, 2013.
- 4 Lurmann, F. W., Brown, S. G., McCarthy, M. C., and Roberts, P. T.: Processes Influencing Secondary  
5 Aerosol Formation in the San Joaquin Valley during Winter, *Journal of the Air & Waste Management*  
6 *Association* (1995), 56, 1679-1693, 2006.
- 7 Marr, L. C., Dzepina, K., Jimenez, J. L., Reisen, F., Bethel, H. L., Arey, J., Gaffney, J. S., Marley, N. A.,  
8 Molina, L. T., and Molina, M. J.: Sources and transformations of particle-bound polycyclic aromatic  
9 hydrocarbons in Mexico City, *Atmos. Chem. Phys.*, 6, 1733-1745, 10.5194/acp-6-1733-2006, 2006.
- 10 Middlebrook, A. M., Bahreini, R., Jimenez, J. L., and Canagaratna, M. R.: Evaluation of Composition-  
11 Dependent Collection Efficiencies for the Aerodyne Aerosol Mass Spectrometer using Field Data,  
12 *Aerosol Science and Technology*, 46, 258-271, 10.1080/02786826.2011.620041, 2012.
- 13 Mohr, C., Huffman, J. A., Cubison, M. J., Aiken, A. C., Docherty, K. S., Kimmel, J. R., Ulbrich, I. M.,  
14 Hannigan, M., and Jimenez, J. L.: Characterization of Primary Organic Aerosol Emissions from Meat  
15 Cooking, Trash Burning, and Motor Vehicles with High-Resolution Aerosol Mass Spectrometry and  
16 Comparison with Ambient and Chamber Observations, *Environmental Science & Technology*, 43,  
17 2443-2449, Doi 10.1021/Es8011518, 2009.
- 18 Mohr, C., DeCarlo, P. F., Heringa, M. F., Chirico, R., Slowik, J. G., Richter, R., Reche, C., Alastuey, A.,  
19 Querol, X., Seco, R., Penuelas, J., Jimenez, J. L., Crippa, M., Zimmermann, R., Baltensperger, U., and  
20 Prevot, A. S. H.: Identification and quantification of organic aerosol from cooking and other sources in  
21 Barcelona using aerosol mass spectrometer data, *Atmospheric Chemistry and Physics*, 12, 1649-1665,  
22 10.5194/acp-12-1649-2012, 2012.
- 23 Morgan, W. T., Allan, J. D., Bower, K. N., Highwood, E. J., Liu, D., McMeeking, G. R., Northway, M. J.,  
24 Williams, P. I., Krejci, R., and Coe, H.: Airborne measurements of the spatial distribution of aerosol  
25 chemical composition across Europe and evolution of the organic fraction, *Atmospheric Chemistry and*  
26 *Physics*, 10, 4065-4083, 10.5194/acp-10-4065-2010, 2010.
- 27 Ng, N. L., Canagaratna, M. R., Zhang, Q., Jimenez, J. L., Tian, J., Ulbrich, I. M., Kroll, J. H., Docherty, K.  
28 S., Chhabra, P. S., Bahreini, R., Murphy, S. M., Seinfeld, J. H., Hildebrandt, L., Donahue, N. M.,  
29 DeCarlo, P. F., Lanz, V. A., Prevot, A. S. H., Dinar, E., Rudich, Y., and Worsnop, D. R.: Organic  
30 aerosol components observed in Northern Hemispheric datasets from Aerosol Mass Spectrometry,  
31 *Atmospheric Chemistry and Physics*, 10, 4625-4641, 10.5194/acp-10-4625-2010, 2010.
- 32 Ng, N. L., Canagaratna, M. R., Jimenez, J. L., Zhang, Q., Ulbrich, I. M., and Worsnop, D. R.: Real-Time  
33 Methods for Estimating Organic Component Mass Concentrations from Aerosol Mass Spectrometer  
34 Data, *Environmental Science & Technology*, 45, 910-916, Doi 10.1021/Es102951k, 2011.
- 35 NIER: Annual report of air quality in Korea 2013. Available at: [http://webbook.me.go.kr/DL-  
36 File/NIER/09/019/5584427.pdf](http://webbook.me.go.kr/DL-File/NIER/09/019/5584427.pdf) 2014. (21/01/2016), 2014.
- 37 Paatero, P., and Tapper, U.: POSITIVE MATRIX FACTORIZATION - A NONNEGATIVE FACTOR  
38 MODEL WITH OPTIMAL UTILIZATION OF ERROR-ESTIMATES OF DATA VALUES,  
39 *Environmetrics*, 5, 111-126, 10.1002/env.3170050203, 1994.
- 40 Parworth, C., Fast, J., Mei, F., Shippert, T., Sivaraman, C., Tilp, A., Watson, T., and Zhang, Q.: Long-term  
41 measurements of submicrometer aerosol chemistry at the southern great plains (SPG) using an aerosol  
42 chemical speciation monitor (ACSM), *Atmospheric Environment*, 106, 12,  
43 10.1016/j.atmosenv.2015.01.060, 2015.



- 1 Petaja, T., Jarvi, L., Kerminen, V. M., Ding, A. J., Sun, J. N., Nie, W., Kujansuu, J., Virkkula, A., Yang,  
2 X. Q., Fu, C. B., Zilitinkevich, S., and Kulmala, M.: Enhanced air pollution via aerosol-boundary layer  
3 feedback in China, *Sci Rep*, 6, 18998, 10.1038/srep18998, 2016.
- 4 Pope III, C. A., and Dockery, D. W.: Health Effects of Fine Particulate Air Pollution: Lines that Connect,  
5 *Journal of the Air & Waste Management Association*, 56, 709-742, 2006.
- 6 Pöschl, U.: Atmospheric Aerosols: Composition, Transformation, Climate and Health Effects, *Angewandte*  
7 *Chemie International Edition*, 44, 7520-7540, 10.1002/anie.200501122, 2005.
- 8 Quan, J., Zhang, Q., He, H., Liu, J., Huang, M., and Jin, H.: Analysis of the formation of fog and haze in  
9 North China Plain (NCP), *Atmospheric Chemistry and Physics*, 11, 8205-8214, 10.5194/acp-11-8205-  
10 2011, 2011.
- 11 Salcedo, D., Onasch, T. B., Dzepina, K., Canagaratna, M. R., Zhang, Q., Huffman, J. A., DeCarlo, P. F.,  
12 Jayne, J. T., Mortimer, P., Worsnop, D. R., Kolb, C. E., Johnson, K. S., Zuberi, B., Marr, L. C.,  
13 Volkamer, R., Molina, L. T., Molina, M. J., Cardenas, B., Bernabe, R. M., Marquez, C., Gaffney, J. S.,  
14 Marley, N. A., Laskin, A., Shutthanandan, V., Xie, Y., Brune, W., Leshner, R., Shirley, T., and Jimenez,  
15 J. L.: Characterization of ambient aerosols in Mexico City during the MCMA-2003 campaign with  
16 Aerosol Mass Spectrometry: results from the CENICA Supersite, *Atmospheric Chemistry and Physics*,  
17 6, 925-946, 2006.
- 18 Seinfeld, J. H., and Pandis, S. N.: *Atmospheric Chemistry and Physics: From Air Pollution to Climate*  
19 *Change*, 2nd ed., John Wiley & Sons, New York, 1232 pp., 2006.
- 20 Setyan, A., Zhang, Q., Merkel, M., Knighton, W. B., Sun, Y., Song, C., Shilling, J. E., Onasch, T. B.,  
21 Herndon, S. C., Worsnop, D. R., Fast, J. D., Zaveri, R. A., Berg, L. K., Wiedensohler, A., Flowers, B.  
22 A., Dubey, M. K., and Subramanian, R.: Characterization of submicron particles influenced by mixed  
23 biogenic and anthropogenic emissions using high-resolution aerosol mass spectrometry: results from  
24 CARES, *Atmospheric Chemistry and Physics*, 12, 8131-8156, 10.5194/acp-12-8131-2012, 2012.
- 25 Simoneit, B. R. T., Rushdi, A. I., bin Abas, M. R., and Didyk, B. M.: Alkyl Amides and Nitriles as Novel  
26 Tracers for Biomass Burning, *Environmental Science & Technology*, 37, 16-21, 10.1021/es020811y,  
27 2003.
- 28 Sun, J., Zhang, Q., Canagaratna, M. R., Zhang, Y., Ng, N. L., Sun, Y., Jayne, J. T., Zhang, X., Zhang, X.,  
29 and Worsnop, D. R.: Highly time- and size-resolved characterization of submicron aerosol particles in  
30 Beijing using an Aerodyne Aerosol Mass Spectrometer, *Atmospheric Environment*, 44, 131-140,  
31 10.1016/j.atmosenv.2009.03.020, 2010.
- 32 Sun, Y., Zhang, Q., Macdonald, A. M., Hayden, K., Li, S. M., Liggio, J., Liu, P. S. K., Anlauf, K. G.,  
33 Leaitch, W. R., Steffen, A., Cubison, M., Worsnop, D. R., van Donkelaar, A., and Martin, R. V.: Size-  
34 resolved aerosol chemistry on Whistler Mountain, Canada with a high-resolution aerosol mass  
35 spectrometer during INTEX-B, *Atmospheric Chemistry and Physics*, 9, 3095-3111, 2009.
- 36 Sun, Y., Wang, Z., Dong, H., Yang, T., Li, J., Pan, X., Chen, P., and Jayne, J. T.: Characterization of  
37 summer organic and inorganic aerosols in Beijing, China with an Aerosol Chemical Speciation  
38 Monitor, *Atmospheric Environment*, 51, 250-259, 10.1016/j.atmosenv.2012.01.013, 2012.
- 39 Sun, Y., Jiang, Q., Wang, Z., Fu, P., Li, J., Yang, T., and Yin, Y.: Investigation of the sources and evolution  
40 processes of severe haze pollution in Beijing in January 2013, *Journal of Geophysical Research-*  
41 *Atmospheres*, 119, 4380-4398, 10.1002/2014jd021641, 2014.
- 42 Sun, Y. L., Zhang, Q., Schwab, J. J., Chen, W. N., Bae, M. S., Lin, Y. C., Hung, H. M., and Demerjian, K.  
43 L.: A case study of aerosol processing and evolution in summer in New York City, *Atmos. Chem.*  
44 *Phys.*, 11, 12737-12750, 10.5194/acp-11-12737-2011, 2011a.



- 1 Sun, Y. L., Zhang, Q., Schwab, J. J., Demerjian, K. L., Chen, W. N., Bae, M. S., Hung, H. M., Hogrefe, O.,  
2 Frank, B., Rattigan, O. V., and Lin, Y. C.: Characterization of the sources and processes of organic and  
3 inorganic aerosols in New York city with a high-resolution time-of-flight aerosol mass spectrometer,  
4 *Atmospheric Chemistry and Physics*, 11, 1581-1602, 10.5194/acp-11-1581-2011, 2011b.
- 5 Ulbrich, I. M., Canagaratna, M. R., Zhang, Q., Worsnop, D. R., and Jimenez, J. L.: Interpretation of organic  
6 components from Positive Matrix Factorization of aerosol mass spectrometric data, *Atmospheric*  
7 *Chemistry and Physics*, 9, 2891-2918, 10.5194/acp-9-2891-2009, 2009.
- 8 Wang, J., Ge, X., Chen, Y., Shen, Y., Zhang, Q., Sun, Y., Xu, J., Ge, S., Yu, H., and Chen, M.: Highly  
9 time-resolved urban aerosol characteristics during springtime in Yangtze River Delta, China: insights  
10 from soot particle aerosol mass spectrometry, *Atmos. Chem. Phys.*, 16, 9109-9127, 10.5194/acp-16-  
11 9109-2016, 2016.
- 12 Weimer, S., Drewnick, F., Hogrefe, O., Schwab, J. J., Rhoads, K., Orsini, D., Canagaratna, M., Worsnop,  
13 D. R., and Demerjian, K. L.: Size-selective nonrefractory ambient aerosol measurements during the  
14 Particulate Matter Technology Assessment and Characterization Study - New York 2004 Winter  
15 Intensive in New York City, *Journal of Geophysical Research-Atmospheres*, 111, 17,  
16 10.1029/2006jd007215, 2006.
- 17 Xu, J., Zhang, Q., Chen, M., Ge, X., Ren, J., and Qin, D.: Chemical composition, sources, and processes of  
18 urban aerosols during summertime in northwest China: insights from high-resolution aerosol mass  
19 spectrometry, *Atmospheric Chemistry and Physics*, 14, 12593-12611, 10.5194/acp-14-12593-2014,  
20 2014.
- 21 Xu, J., Shi, J., Zhang, Q., Ge, X., Canonaco, F., Prévôt, A. S. H., Vonwiller, M., Szidat, S., Ge, J., Ma, J.,  
22 An, Y., Kang, S., and Qin, D.: Wintertime organic and inorganic aerosols in Lanzhou, China: Sources,  
23 processes and comparison with the results during summer, *Atmospheric Chemistry and Physics*  
24 *Discussions*, 1-52, 10.5194/acp-2016-278, 2016.
- 25 Xu, L., Guo, H., Boyd, C. M., Klein, M., Bougiatioti, A., Cerully, K. M., Hite, J. R., Isaacman-VanWertz,  
26 G., Kreisberg, N. M., Knote, C., Olson, K., Koss, A., Goldstein, A. H., Hering, S. V., de Gouw, J.,  
27 Baumann, K., Lee, S.-H., Nenes, A., Weber, R. J., and Ng, N. L.: Effects of anthropogenic emissions  
28 on aerosol formation from isoprene and monoterpenes in the southeastern United States, *Proceedings*  
29 *of the National Academy of Sciences of the United States of America*, 112, 37-42,  
30 10.1073/pnas.1417609112, 2015.
- 31 Young, D. E., Kim, H., Parworth, C., Zhou, S., Zhang, X., Cappa, C. D., Seco, R., Kim, S., and Zhang, Q.:  
32 Influences of emission sources and meteorology on aerosol chemistry in a polluted urban environment:  
33 results from DISCOVER-AQ California, *Atmos. Chem. Phys.*, 16, 5427-5451, 10.5194/acp-16-5427-  
34 2016, 2016.
- 35 Zhang, J. K., Sun, Y., Liu, Z. R., Ji, D. S., Hu, B., Liu, Q., and Wang, Y. S.: Characterization of submicron  
36 aerosols during a month of serious pollution in Beijing, 2013, *Atmospheric Chemistry and Physics*, 14,  
37 2887-2903, 10.5194/acp-14-2887-2014, 2014.
- 38 Zhang, Q., Alfarra, M. R., Worsnop, D. R., Allan, J. D., Coe, H., Canagaratna, M. R., and Jimenez, J. L.:  
39 Deconvolution and quantification of hydrocarbon-like and oxygenated organic aerosols based on  
40 aerosol mass spectrometry, *Environmental Science & Technology*, 39, 4938-4952, 10.1021/Es0485681,  
41 2005a.
- 42 Zhang, Q., Canagaratna, M. R., Jayne, J. T., Worsnop, D. R., and Jimenez, J. L.: Time- and size-resolved  
43 chemical composition of submicron particles in Pittsburgh: Implications for aerosol sources and  
44 processes, *Journal of Geophysical Research-Atmospheres*, 110, 10.1029/2004jd004649, 2005b.
- 45 Zhang, Q., Jimenez, J. L., Canagaratna, M. R., Allan, J. D., Coe, H., Ulbrich, I., Alfarra, M. R., Takami,  
46 A., Middlebrook, A. M., Sun, Y. L., Dzepina, K., Dunlea, E., Docherty, K., DeCarlo, P. F., Salcedo,



- 1 D., Onasch, T., Jayne, J. T., Miyoshi, T., Shimono, A., Hatakeyama, S., Takegawa, N., Kondo, Y.,  
2 Schneider, J., Drewnick, F., Borrmann, S., Weimer, S., Demerjian, K., Williams, P., Bower, K.,  
3 Bahreini, R., Cottrell, L., Griffin, R. J., Rautiainen, J., Sun, J. Y., Zhang, Y. M., and Worsnop, D. R.:  
4 Ubiquity and dominance of oxygenated species in organic aerosols in anthropogenically-influenced  
5 Northern Hemisphere midlatitudes, *Geophysical Research Letters*, 34, L13801, Artn L13801, Doi  
6 10.1029/2007gl029979, 2007a.
- 7 Zhang, Q., Jimenez, J. L., Worsnop, D. R., and Canagaratna, M.: A case study of urban particle acidity and  
8 its influence on secondary organic aerosol, *Environmental Science & Technology*, 41, 3213-3219,  
9 10.1021/Es061812j, 2007b.
- 10 Zhang, Q., Jimenez, J. L., Canagaratna, M. R., Ulbrich, I. M., Ng, N. L., Worsnop, D. R., and Sun, Y.:  
11 Understanding atmospheric organic aerosols via factor analysis of aerosol mass spectrometry: a review,  
12 *Analytical and bioanalytical chemistry*, 401, 3045-3067, 10.1007/s00216-011-5355-y, 2011.
- 13 Zhang, Y. J., Tang, L. L., Wang, Z., Yu, H. X., Sun, Y. L., Liu, D., Qin, W., Canonaco, F., Prevot, A. S.  
14 H., Zhang, H. L., and Zhou, H. C.: Insights into characteristics, sources, and evolution of submicron  
15 aerosols during harvest seasons in the Yangtze River delta region, China, *Atmospheric Chemistry and  
16 Physics*, 15, 1331-1349, 10.5194/acp-15-1331-2015, 2015.
- 17 Zhao, Y., Hu, M., Slanina, S., and Zhang, Y.: Chemical compositions of fine particulate organic matter  
18 emitted from Chinese cooking, *Environmental Science & Technology*, 41, 99-105, 10.1021/es0614518,  
19 2007.
- 20 Zhou, S., Collier, S., Jaffe, D. A., Briggs, N. L., Hee, J., Sedlacek Iii, A. J., Kleinman, L., Onasch, T. B.,  
21 and Zhang, Q.: Regional Influence of Wildfires on Aerosol Chemistry in the Western US and Insights  
22 into Atmospheric Aging of Biomass Burning Organic Aerosol, *Atmos. Chem. Phys. Discuss.*, 2016, 1-  
23 27, 10.5194/acp-2016-823, 2016a.
- 24 Zhou, S., Collier, S., Xu, J. Z., Mei, F., Wang, J., Lee, Y. N., Sedlacek, A. J., Springston, S. R., Sun, Y. L.,  
25 and Zhang, Q.: Influences of upwind emission sources and atmospheric processing on aerosol  
26 chemistry and properties at a rural location in the Northeastern US, *Journal of Geophysical Research-  
27 Atmospheres*, 121, 6049-6065, 10.1002/2015jd024568, 2016b.
- 28
- 29



## 1 Tables

2 **Table 1.** Average ( $\pm 1$  standard deviation), minimum and maximum concentrations of the  
 3 particulate matter (PM<sub>1</sub>) species and the total PM<sub>1</sub> mass over the whole campaign, and the average  
 4 contribution of each of the PM<sub>1</sub> species to the total PM<sub>1</sub> mass.

	Average conc. $\pm$ one standard deviation ( $\mu\text{g m}^{-3}$ )	Minimum conc. ( $\mu\text{g m}^{-3}$ )	Maximum conc. ( $\mu\text{g m}^{-3}$ )	Fraction of total PM <sub>1</sub> (%)	Detection limit (3min/ 6min) ( $\mu\text{g m}^{-3}$ )
Organics	12.1 $\pm$ 8.03	1.32	53.1	44	0.03/0.02
Nitrate	6.55 $\pm$ 5.12	0.18	26.0	24	0.01/0.01
Sulfate	2.87 $\pm$ 2.00	0.38	10.7	10	0.01/0.01
Ammonium	3.11 $\pm$ 2.20	0.21	10.5	12	0.02/0.01
Chloride	0.26 $\pm$ 0.32	0	2.91	1	0.01/0.01
Black carbon	2.54 $\pm$ 1.66	0	10.1	9	0.1/0.05
Total PM <sub>1</sub>	27.5 $\pm$ 17.2	1.32	90.7	-	0.04/0.03

5



1 **Table 2.** Correlation coefficient (Pearson's  $r$ ) for the linear regressions between organic aerosol  
 2 (OA) factors (including the sum of primary factors (primary OA (POA) = hydrocarbon like OA  
 3 (HOA) + cooking OA (COA) + biomass burning OA (BBOA)), as well as the sum of the oxidized  
 4 factors (oxidized OA (OOA) = semi-volatile OOA (SV-OOA) + low volatile (LV-OOA)), and  
 5 various particle- and gas-phase species, and ions.

$r$	HOA	COA	BBOA	POA (HOA+ COA+BBOA)	SV-OOA	LV-OOA	OOA (SV-OOA+ LV-OOA)
Nitrate	0.32	0.30	0.41	0.43	<b>0.87</b>	0.63	<b>0.87</b>
Sulfate	0.25	0.17	0.09	0.23	<b>0.71</b>	<b>0.80</b>	<b>0.88</b>
Ammonium	0.41	0.30	0.37	0.45	<b>0.87</b>	0.69	<b>0.90</b>
Chloride	<b>0.80</b>	0.30	0.50	0.68	0.50	0.13	0.36
K (AMS)	0.59	0.60	0.63	<b>0.77</b>	0.61	0.22	0.47
Primary pollutants							
PAH	0.48	0.60	<b>0.90</b>	<b>0.81</b>	0.37	-0.11	0.14
BC	0.63	0.56	<b>0.82</b>	<b>0.83</b>	0.69	0.18	0.50
CO	0.52	0.54	0.62	<b>0.74</b>	0.61	0.29	0.51
NO <sub>2</sub>	0.45	0.64	0.61	<b>0.72</b>	0.57	0.20	0.44
AMS tracer ions ( $m/z$ value)							
CO <sub>2</sub> <sup>+</sup> (44)	0.32	0.38	0.41	0.47	<b>0.84</b>	<b>0.75</b>	<b>0.92</b>
C <sub>2</sub> H <sub>5</sub> N <sup>+</sup> (43)	0.46	0.52	0.48	0.62	0.52	0.35	0.50
C <sub>2</sub> H <sub>4</sub> O <sub>2</sub> <sup>+</sup> (60)	<b>0.70</b>	0.66	0.85	<b>0.92</b>	0.67	0.10	0.44
C <sub>3</sub> H <sub>5</sub> O <sub>2</sub> <sup>+</sup> (73)	<b>0.71</b>	<b>0.76</b>	<b>0.74</b>	<b>0.94</b>	<b>0.66</b>	0.15	0.46
C <sub>3</sub> H <sub>3</sub> O <sup>+</sup> (55)	0.55	<b>0.86</b>	0.64	<b>0.88</b>	0.66	0.24	0.51
C <sub>3</sub> H <sub>7</sub> <sup>+</sup> (43)	<b>0.91</b>	<b>0.69</b>	0.63	<b>0.96</b>	0.46	0.02	0.27
C <sub>3</sub> H <sub>7</sub> N <sup>+</sup> (57)	0.60	0.57	0.56	<b>0.74</b>	<b>0.78</b>	0.33	0.63
C <sub>4</sub> H <sub>7</sub> <sup>+</sup> (55)	<b>0.85</b>	<b>0.78</b>	0.65	<b>0.98</b>	0.49	0.04	0.30
C <sub>4</sub> H <sub>9</sub> <sup>+</sup> (43)	<b>0.95</b>	0.62	0.61	<b>0.94</b>	0.42	0.00	0.24
C <sub>5</sub> H <sub>11</sub> <sup>+</sup> (57)	<b>0.96</b>	0.59	0.60	<b>0.92</b>	0.41	-0.01	0.23
C <sub>5</sub> H <sub>8</sub> O <sup>+</sup> (84)	0.58	<b>0.93</b>	0.54	<b>0.90</b>	0.50	0.09	0.33
C <sub>6</sub> H <sub>10</sub> O <sup>+</sup> (98)	0.57	<b>0.95</b>	0.51	<b>0.89</b>	0.41	0.02	0.24
C <sub>7</sub> H <sub>12</sub> O <sup>+</sup> (112)	0.57	<b>0.89</b>	0.58	<b>0.88</b>	0.53	0.09	0.35
C <sub>9</sub> H <sub>7</sub> <sup>+</sup> (115)	<b>0.82</b>	<b>0.74</b>	<b>0.72</b>	<b>0.96</b>	0.18	-0.05	0.10
CHN <sup>+</sup> (27)	0.47	0.47	0.58	0.63	<b>0.73</b>	0.53	<b>0.73</b>
CN <sup>+</sup> (26)	0.35	0.35	0.46	0.48	0.57	0.42	0.57
CH <sub>2</sub> SO <sub>2</sub> <sup>+</sup> (77)	0.30	0.24	0.37	0.37	<b>0.83</b>	0.53	<b>0.79</b>
CH <sub>3</sub> SO <sub>2</sub> <sup>+</sup> (78)	0.37	0.27	0.41	0.44	<b>0.91</b>	0.54	<b>0.83</b>

6 BC, black carbon; AMS, aerosol mass spectrometer; PAH, polycyclic aromatic hydrocarbons

7 Value that are  $r > 0.7$  are boldfaced



1 **Table 3.** Comparison of aerosol properties and meteorological parameters between the high  
 2 loading and low loading periods.

	High PM loading	Low PM loading
Average non-refractory submicrometer particulate matter (NR-PM <sub>1</sub> ) mass concentration (μg m <sup>-3</sup> ) (Average ± 1σ)	43.6 ± 2.4	12.6 ± 7.1
O/C (H/C) ratio*	0.36 (1.82)	0.41 (1.75)
Gas conc.(CO (ppm) and /NO <sub>2</sub> /O <sub>3</sub> /SO <sub>2</sub> (ppb))	1.2/56/61/7.5	0.5/30/18.4/6.4
Temperature (°C) (average ± 1σ)	2.5 ± 3.4	-2.8 ± 4.4
RH (%) (average ± 1σ)	71 ± 15	50 ± 12

3 \*calculated using the improved Canagaratna-ambient method (Canagaratna et al., 2015).

4 PM, particulate matter; NR-PM<sub>1</sub>, non-refractory submicrometer particulate matter; RH, relative humidity

5



1 Figures

2

3

4

5

6

7

8

9

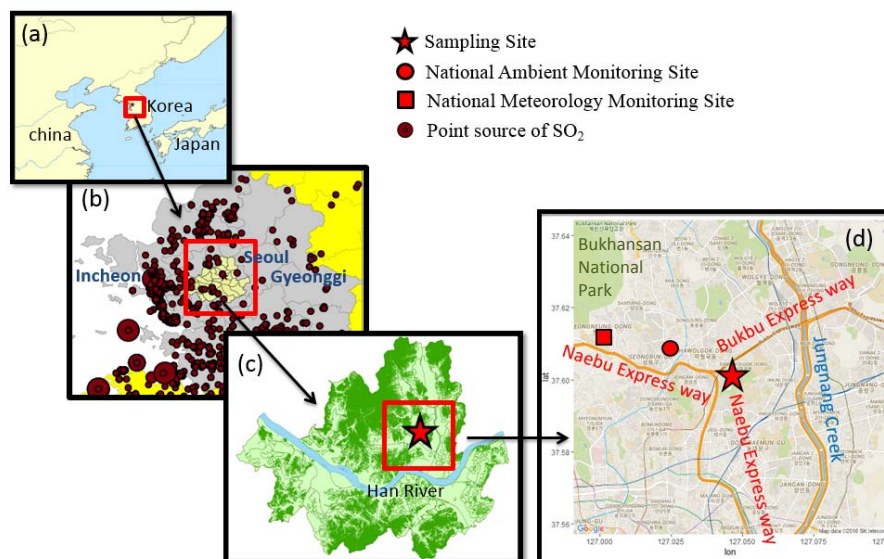
10

11

12

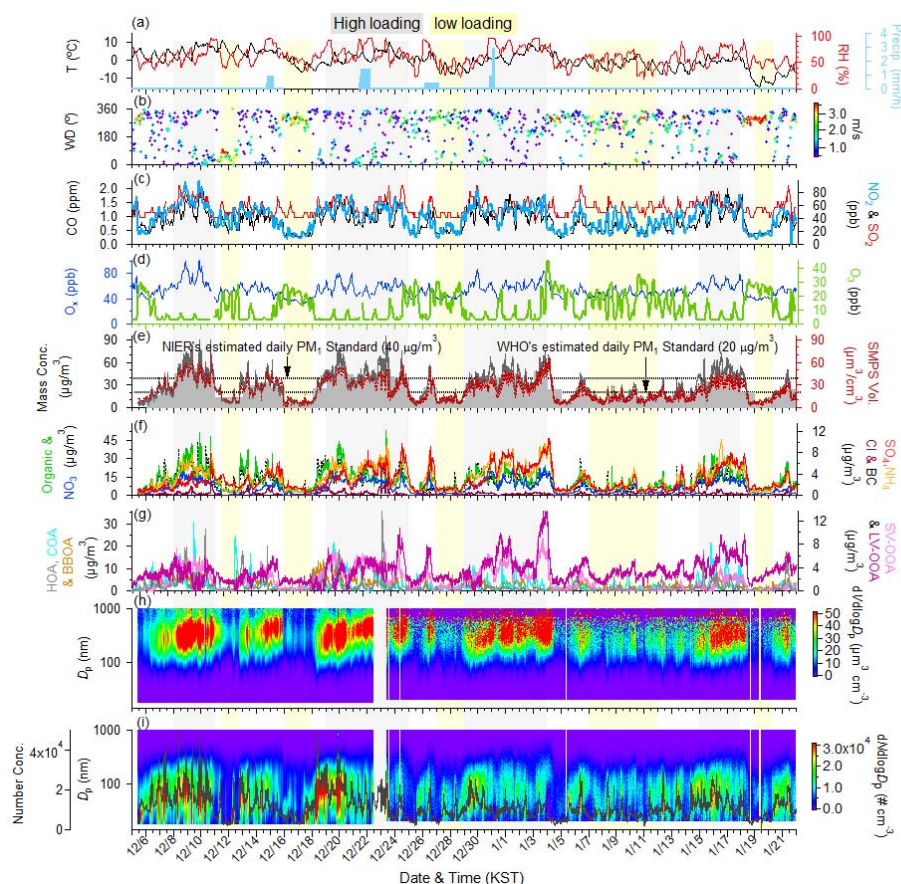
13

14



15 **Figure 1.** (a) The map of Korea, showing the location between China and Japan; (b) Seoul (light  
16 yellow) surrounded by other nearby cities including Incheon and Gyeonggi (Grey area) where  
17 industrial facilities are located (west) and agricultural areas are sporadically located surrounding  
18 Seoul. Location of point source of SO<sub>2</sub> are indicated by dark red circles (Size: Concentration).  
19 Agricultural areas are sporadically located at East; (c) The location of sampling site in Seoul which  
20 is at the north-east of the city center and north of Han river; (d) The indications of sampling site.  
21 Next to sampling site, Bukbu express highway is located and residential and commercial areas are  
22 surrounding the sampling site.

23



1

2 **Figure 2.** Overview of the temporal variations of submicron aerosols at the Korea Institute of  
 3 Science and Technology (KIST) in Seoul from December 8, 2015 to January 21, 2016: **(a)** Time  
 4 series of ambient air temperature (T), relative humidity (RH), solar radiation (SR), and  
 5 precipitation (Precip.); **(b)** Time series of wind direction (WD), with colors showing different wind  
 6 speeds (WS); **(c)** Time series of CO,SO<sub>2</sub>, and NO<sub>2</sub>; **(d)** Time series of O<sub>x</sub> (NO<sub>2</sub> + O<sub>3</sub>) and O<sub>3</sub>; **(e)**  
 7 Time series of total particulate matter (PM<sub>1</sub>),scanning mobility particle sizer (SMPS) volume  
 8 concentrations Also shown are the 24 h averaged PM<sub>1</sub>+BC with bars. Estimated NIER's and  
 9 WHO's daily PM<sub>1</sub> standards (40 µg/m<sup>3</sup> and 20 µg/m<sup>3</sup>, respectively) are also shown with dashed  
 10 line for the comparisons; **(f)** Time series of the organic aerosols (Org.), nitrate (NO<sub>3</sub><sup>-</sup>), sulfate  
 11 (SO<sub>4</sub><sup>2-</sup>), ammonium (NH<sub>4</sub><sup>+</sup>), chloride (Cl<sup>-</sup>), and BC; **(g)** Time series of the total organic aerosol



1 (OA) of the five factors derived from the positive matrix factorization (PMF) analysis (see section  
2 3.3) (**h,i**) Particle volume and number size distributions by SMPS. Shaded regions indicate the  
3 persistent (> 2days) high loading (gray) and low loading (yellow) periods when daily average conc.  
4 > 30  $\mu\text{g}/\text{m}^3$  and <14  $\mu\text{g}/\text{m}^3$ , respectively.

5

6

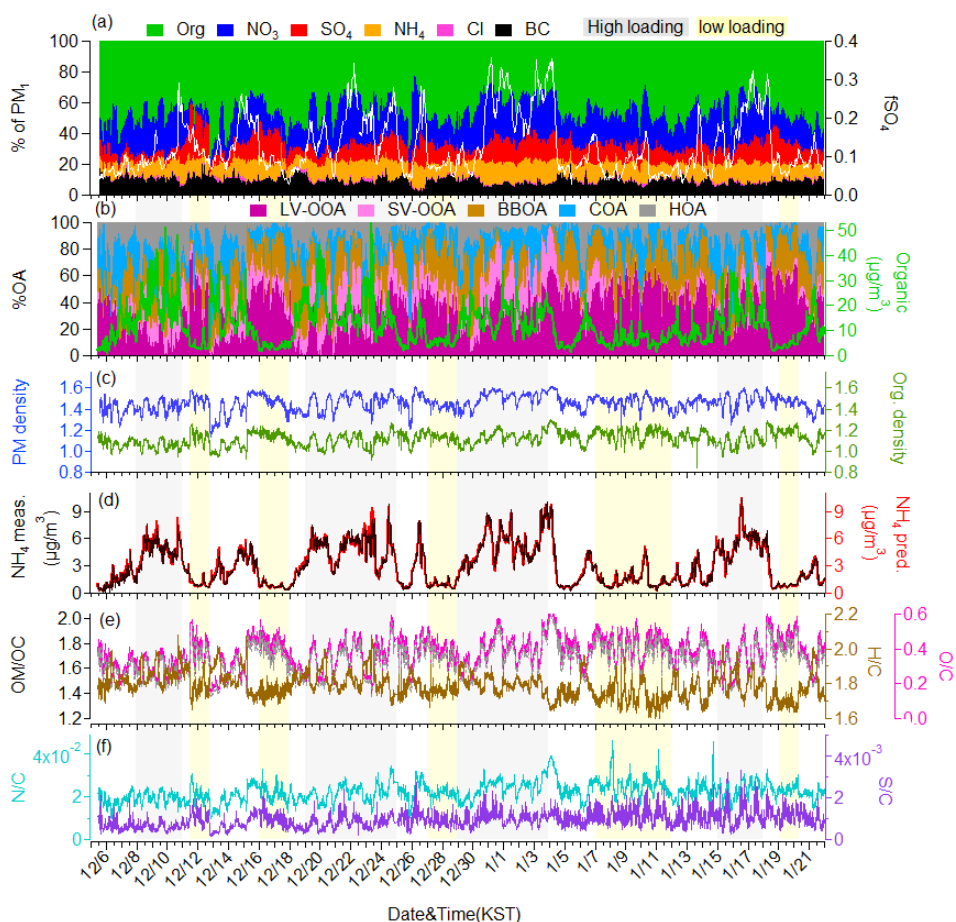
7

8

9

10

11



1

2 **Figure 3.** Overview of the chemical composition of submicron aerosols at the Korea Institute of  
 3 Science and Technology (KIST) in Seoul from December 8, 2015 to January 21, 2016: (a) Time  
 4 series of the mass fractional contribution of organic aerosols (Org.), nitrate ( $\text{NO}_3^-$ ), sulfate ( $\text{SO}_4^{2-}$ )  
 5 ), ammonium ( $\text{NH}_4^+$ ), chloride ( $\text{Cl}^-$ ), and BC to total  $\text{PM}_{10}$ . Also shown is the time series of  $f_{\text{SO}_4}$   
 6 (ratio of  $\text{SO}_4^{2-}/(\text{SO}_2 + \text{SO}_4^{2-})$ ) with the fraction of  $\text{SO}_4^{2-}$  to the concentration of  $f$ ; (b) Time series of  
 7 the mass fractional contribution to total organic aerosol (OA) of the five factors derived from the  
 8 positive matrix factorization (PMF) analysis (see section 3.3), and the time series of the organic  
 9 aerosols; (c) Time series of the organic density estimate using the method reported in (Kuwata et  
 10 al., 2012) with bulk aerosol density using the organic density estimated in this figure; (d) Time



1 series of the measured and predicted  $\text{NH}_4^+$  concentrations; **(e, f)** organic matter to organic carbon  
 2 (OM/OC), oxygen to carbon (O/C), hydrogen to carbon (H/C), nitrogen to carbon (N/C), and sulfur  
 3 to carbon (S/C) ratios of OA, where the O/C, H/C and OM/OC elemental ratios were determined  
 4 using the updated method (Canagaratna et al., 2015).

5

6

7

8

9

10

11

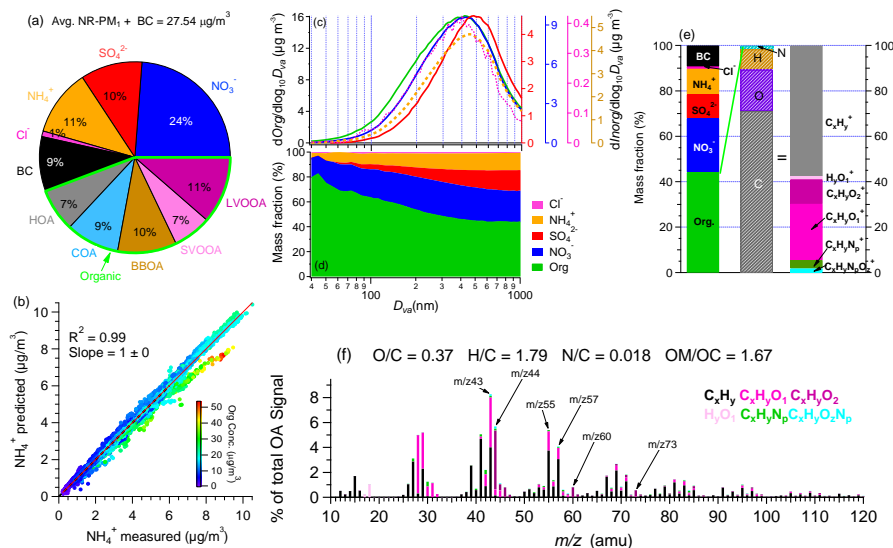
12

13

14

15

16



17 **Figure 4.** **(a)** Average compositional pie chart of PM<sub>1</sub> species (non-refractory-PM<sub>1</sub> plus black  
 18 carbon (BC)) and each of the OA factors over the whole campaign. The green outline indicates the  
 19 fraction of total OA; **(b)** Scatterplot that compares predicted  $\text{NH}_4^+$  versus measured  $\text{NH}_4^+$   
 20 concentrations. The predicted values were calculated assuming full neutralization of the anions  
 21 (e.g., sulfate, nitrate, and chloride). The data points are colored by organic concentrations.; **(c)**  
 22 Campaign-averaged size distributions for individual NR-PM<sub>1</sub> species; **(d)** Averaged mass  
 23 fractional contributions of each NR-PM<sub>1</sub> species to the total NR-PM<sub>1</sub> mass as a function of size. ;  
 24 **(e)** Overview of the average PM<sub>1</sub> and OA compositions in Seoul during winter; **(f)** Average high-  
 25 resolution mass spectrum of OA colored by the different ion families. The average elemental ratios  
 26 for the OA fraction are described.

27



1

2

3

4

5

6

7

8

9

10

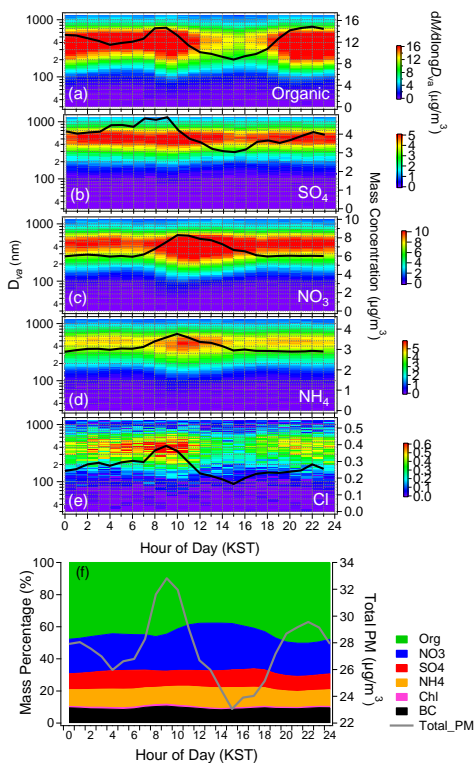
11

12

13

14

15



16 **Figure 5. (a–e)** One-hour averaged diurnal profiles of mass-based size distributions of each of the  
17 non-refractory submicrometer particulate matter (NR-PM<sub>1</sub>) species colored by their mass  
18 concentration (left axis;  $D_{va}$ , vacuum aerodynamic diameter) and average diurnal profiles of each  
19 of the PM<sub>1</sub> species (right axis); **(f)** Average diurnal mass fractional contribution of each of PM<sub>1</sub>  
20 species to the total PM<sub>1</sub> diurnal mass and the total PM<sub>1</sub> mass loading

21



1  
2  
3  
4  
5  
6  
7  
8  
9  
10  
11  
12  
13  
14  
15  
16  
17  
18  
19  
20  
21  
22  
23  
24  
25  
26  
27  
28  
29  
30  
31  
32  
33  
34  
35  
36  
37  
38  
39  
40  
41  
42  
43  
44  
45

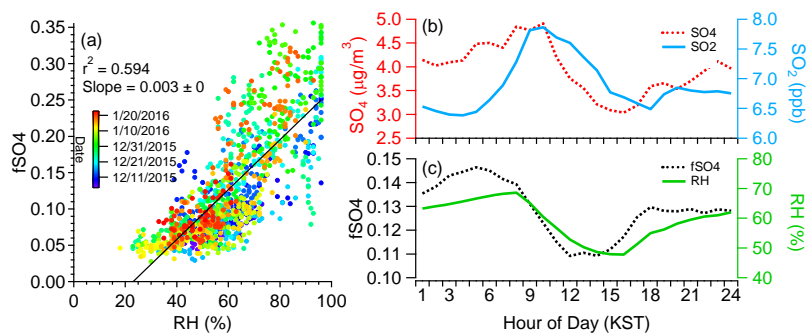
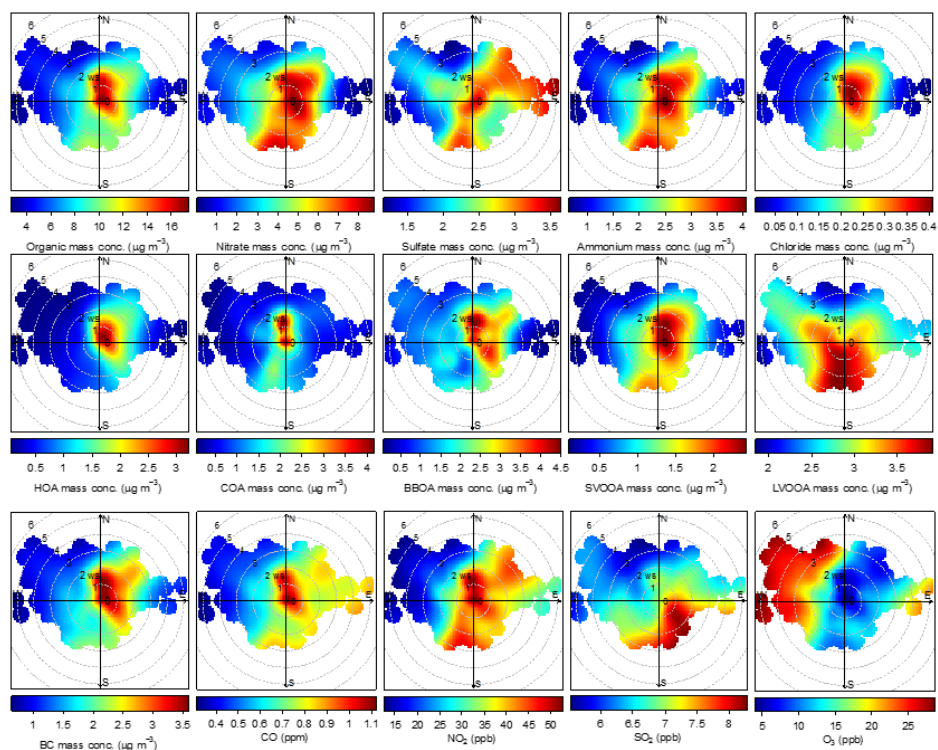


**Figure 6.** (a) Scatterplot of the variations of fSO<sub>4</sub> ratios as a function of RH (b) One-hour averaged diurnal profiles of SO<sub>2</sub> and SO<sub>4</sub> and (c) One-hour averaged diurnal profiles of fSO<sub>4</sub> and RH.



1  
2  
3  
4



5

6

7 **Figure 7.** Polar plots of hourly averaged PM<sub>1</sub> species concentrations (top row), mass  
8 concentrations of the five OA factors identified from PMF analysis (middle row), and the mixing  
9 ratios of various gas phase species as a function of WS and direction.

10

11

12

13

14

15



1  
2  
3  
4  
5  
6  
7  
8  
9  
10  
11  
12  
13  
14  
15  
16  
17  
18  
19  
20  
21  
22  
23  
24  
25

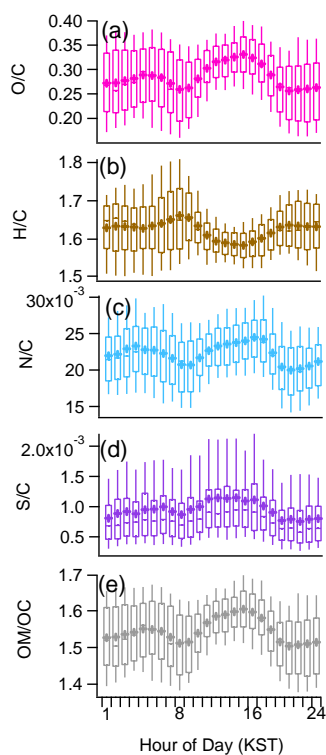
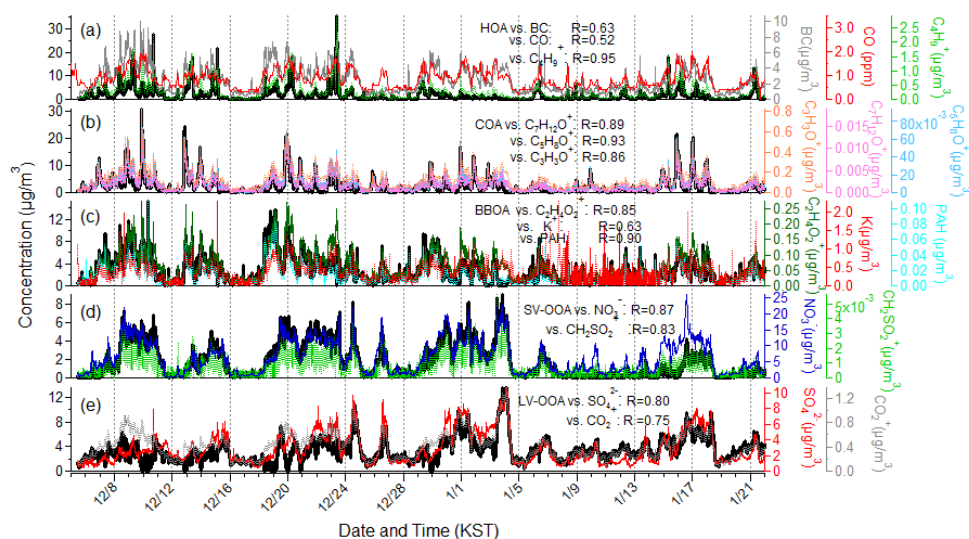


**Figure 8.** (a–e) Average diurnal profiles of the organic matter to organic carbon (OM/OC), oxygen to carbon (O/C), hydrogen to carbon (H/C), nitrogen to carbon (N/C), and sulfur to carbon (S/C) ratios of OA, where the O/C, H/C and OM/OC elemental ratios were determined using the updated method (Canagaratna et al., 2015).



1  
2



3  
4  
5  
6  
7  
8  
9  
10  
11  
12  
13  
14  
15  
16  
17

**Figure 9.** Overview of the results from PMF analysis including high-resolution mass spectra of the Time series of each of the OA factors and various tracer species.



1  
2  
3  
4  
5  
6  
7  
8  
9  
10  
11  
12  
13  
14  
15  
16  
17  
18  
19  
20  
21  
22  
23  
24  
25  
26  
27  
28  
29  
30  
31  
32  
33  
34  
35  
36  
37  
38  
39  
40  
41

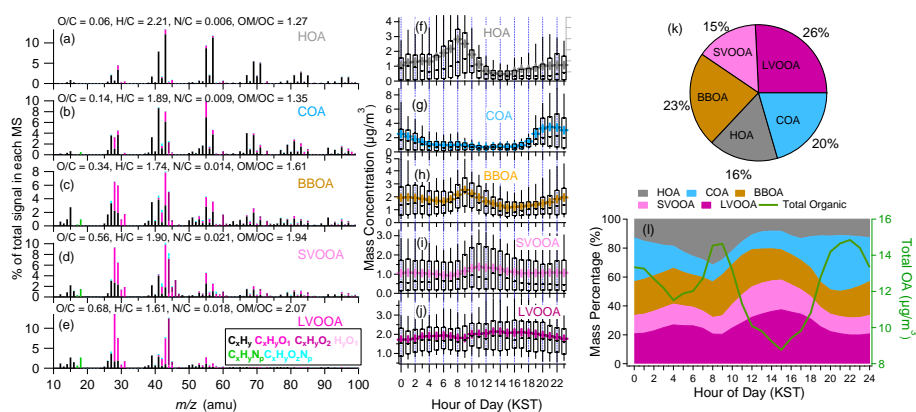


**Figure 10.** Overview of the results from PMF analysis including high-resolution mass spectra of the (a) Hydrocarbon-like organic aerosol (HOA), (b) Cooking OA (COA), (c) Biomass burning OA (BBOA), (d) Semi volatile oxygenated OA (SV-OOA), and (e) Low volatility oxygenated OA (LV-OOA) colored by different ion families; (f–i) Average diurnal profiles of each of the OA factors (the 90<sup>th</sup> and 10<sup>th</sup> percentiles are denoted by the whiskers above and below the boxes, the 75<sup>th</sup> and 25<sup>th</sup> percentiles are denoted by the top and bottom of the boxes, the median values are denoted by the horizontal line within the box, and the mean values are denoted by the colored markers); (k) Compositional pie chart of the average fractional contribution of each of the OA factors to the total OA over the campaign; (l) Average diurnal mass fractional contribution of each of the OA factors to the total OA diurnal mass and the total OA mass loading.



1  
2  
3  
4  
5  
6  
7  
8  
9  
10  
11  
12  
13  
14  
15  
16  
17  
18  
19  
20  
21  
22  
23  
24  
25  
26  
27  
28  
29  
30  
31  
32  
33  
34  
35  
36

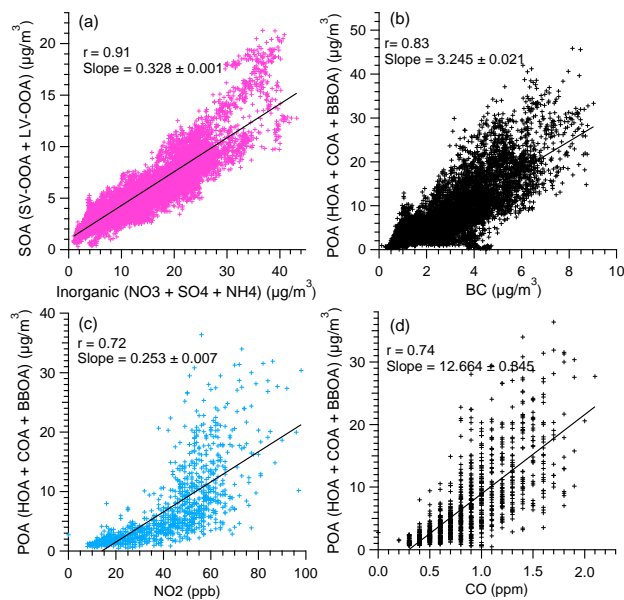


**Figure 11.** Scatterplot between: (a) SOA and sum of inorganic ( $\text{NO}_3 + \text{SO}_4 + \text{NH}_4$ ) (b) POA and BC; (c) POA and  $\text{NO}_2$ ; and (d) POA and CO



1  
 2  
 3  
 4  
 5  
 6  
 7  
 8  
 9  
 10  
 11  
 12  
 13  
 14  
 15  
 16  
 17  
 18  
 19  
 20  
 21  
 22  
 23  
 24  
 25

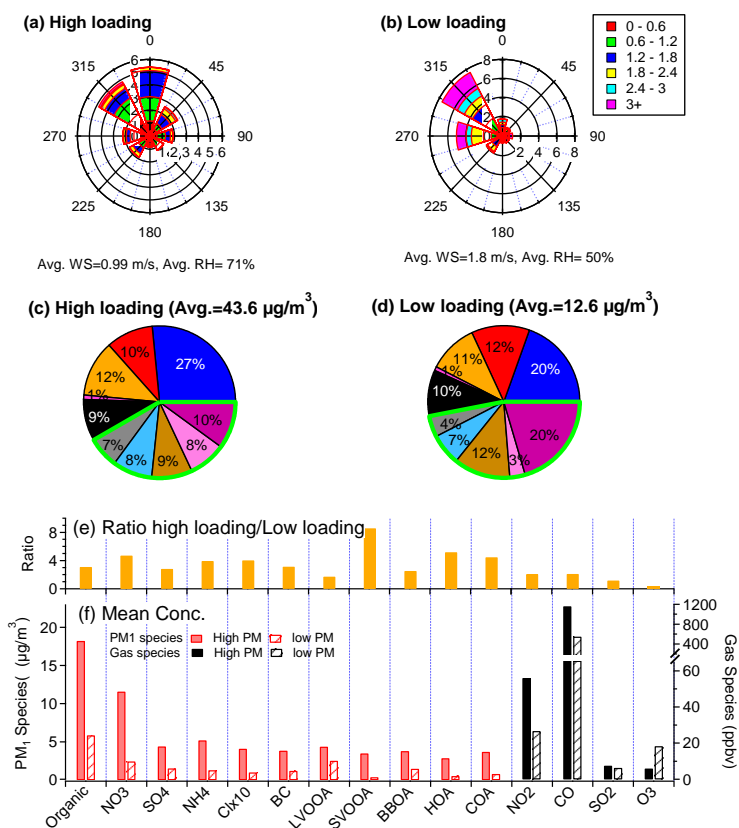


**Figure 12.** Comparisons of averaged properties measured during high particulate matter (PM), loading and low PM loading periods; **(a,b)** Wind rose plots, colored by wind speed for each different period; **(c,d)** fractional contributions of each species to the total PM<sub>1</sub> (non-refractory-PM<sub>1</sub> plus BC) mass; **(e)** ratios of absolute concentrations of each PM<sub>1</sub> and gas species during high loading and low loading periods; **(f)** Comparisons of averaged absolute concentrations of PM<sub>1</sub> species and gaseous pollutants for each different period.



1

2

3

4

5

6

7

8

9

10

11

12

13

14

15

16

17

18

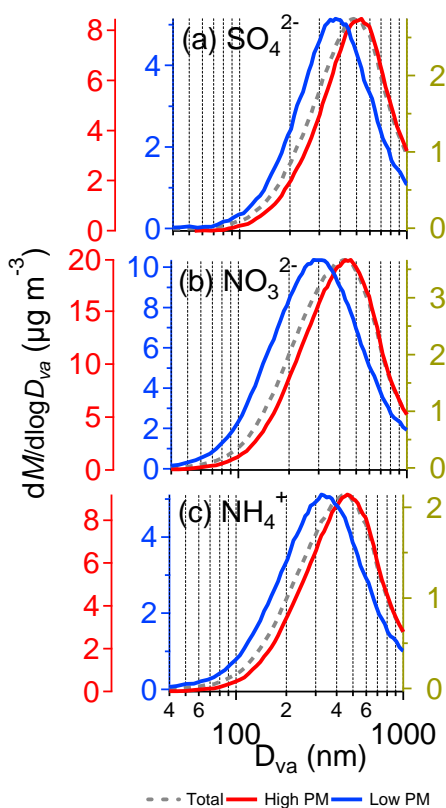
19

20

21

22 **Figure 13.** Averaged mass-based size distributions of (a) sulfate, (b) nitrate, and (c) ammonium  
23 during the entire, high PM, and low PM periods as marked in Fig. 2 and 3.

24





1  
 2  
 3  
 4  
 5  
 6  
 7  
 8  
 9  
 10  
 11  
 12  
 13  
 14  
 15  
 16  
 17  
 18  
 19  
 20  
 21  
 22  
 23

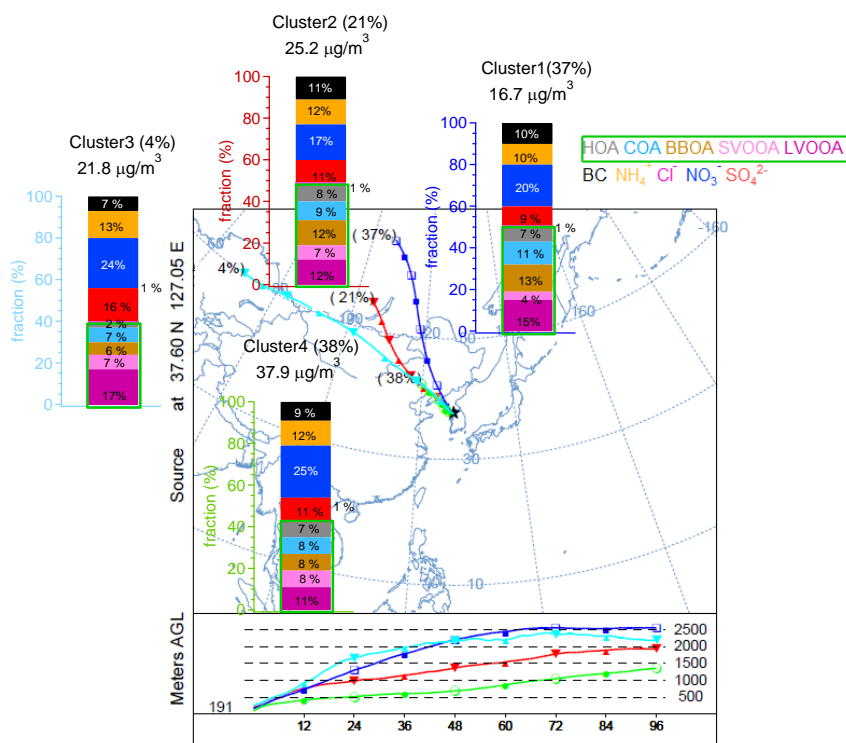


**Figure 14.** Averaged compositional bar graph of PM<sub>1</sub> species (non-refractory-PM<sub>1</sub> plus black carbon (BC)) and each of the OA factors in different clusters from four cluster solution at arriving 500 m height.